Palmitic acid damages gut epithelium integrity and initiates inflammatory cytokine production

Sara Ghezzal, Bárbara Graziela Postal, Elodie Quévrain, Loic Brot, Philippe Seksik, Armelle Leturque, Sophie Thenet, Véronique Carriere

Palmitic acid damages gut epithelium integrity and initiates inflammatory cytokine production

Sara Ghezzal[a,1], Barbara Graziela Postal[a,1], Elodie Quevrain[c], Loic Brot[d], Philippe Seksik[d,e], Armelle Leturque[a], Sophie Thenet[a,b,2], Véronique Carrière[a,2,*]

[1,2]These authors contributed equally to this work

[a] Sorbonne Université, INSERM, Université Paris Descartes Paris 5, CNRS, Centre de Recherche des Cordeliers, F-75006 Paris, France

[b] EPHE, PSL Research University, F-75006 Paris, France

[c] Laboratoire des Biomolécules, LBM, Département de chimie, Ecole Normale Supérieure, ENS, PSL University, Sorbonne Université, CNRS, F-75005 Paris, France.

[d] Sorbonne Université, Centre de Recherche de Saint Antoine INSERM, UMRS 938, F-75012 Paris, France

[e] Service de Gastroentérologie & Nutrition, Hôpital Saint-Antoine, APHP, F-75012 Paris, France

*****To whom correspondence should be addressed (present address): Dr Véronique Carrière, UMRS 938, Centre de Recherche de Saint-Antoine, 27 rue de Chaligny, 75012, Paris, France, Phone: 33140011389, Email: veronique.carriere@sorbonne-universite.fr

Keywords: fatty acid, intestine, inflammation, cytokine, cell-cell junction, gut permeability.

Abbreviations:

DAPI: 4’,6-diamidino-2-phenylindole
DDIT3: DNA Damage Inducible Transcript 3
DSS : dextran sodium sulfate
DTT: dithiothreitol
EGTA: ethylene glycol tetraacetic acid
ELISA : enzyme-linked immunosorbent assay
ER: endoplasmic reticulum
EtOH : ethanol
HSPA5: Heat Shock Protein Family A (Hsp70) Member 5
OA: oleic acid
PA: palmitic acid
TEER: Transepithelial electrical resistance
XBP1: X-box binding protein-1
ZO-1: zonula occludens-1

Abstract

The mechanisms leading to the low-grade inflammation observed during obesity are not fully understood. Seeking the initiating events, we tested the hypothesis that the intestine could be damaged by repeated lipid supply and therefore participate in inflammation. In mice, 1–5 palm oil gavages increased intestinal permeability via decreased expression and mislocalization of junctional proteins at the cell–cell contacts; altered the intestinal bacterial species by decreasing the abundance of *Akkermansia muciniphila*, segmented filamentous bacteria, and *Clostridium leptum*; and increased inflammatory cytokine expression. This was further studied in human intestinal epithelial Caco-2/TC7 cells using the two main components of palm oil, i.e., palmitic and oleic acid. Saturated palmitic acid impaired paracellular permeability and junctional protein localization, and induced inflammatory cytokine expression in the cells, but unsaturated oleic acid did not. Inhibiting *de novo* ceramide synthesis prevented part of these effects. Altogether, our data show that short exposure to palm oil or palmitic acid induces intestinal dysfunctions targeting barrier integrity and inflammation. Excessive palm oil consumption could be an early player in the gut alterations observed in metabolic diseases.

Highlights

- Palm oil gavages damage the intestinal barrier.
- Bacterial species in mice are changed after four palm oil gavages.
- Palmitic acid impairs paracellular permeability and cell-cell junctions.
- Palmitic acid modifies cytokine expression profile in intestinal epithelial cells.
- De novo synthesis of ceramide reproduces palmitic acid deleterious effects.

1. Introduction

Obesity is the result of an energy imbalance between calories consumed and calories expended, and its increasing incidence is associated with changes in eating habits. Obesity is associated with systemic and tissue low-grade inflammation, which contributes to the development of insulin resistance and increased cardiovascular disease risk [1, 2]. While adipose tissue inflammation has been described as an important actor in maintenance of the inflammatory state once obesity is established [1], its origin remains undetermined.

The subclinical systemic inflammation observed during obesity has been attributed to the immune response to increased circulating levels of lipopolysaccharides (LPS) from the gram-negative bacterial cell wall, termed metabolic endotoxemia [3]. The passage of bacterial fragments into the blood through the intestinal mucosa emphasizes the importance of the intestinal epithelial barrier in this process [3-5]. In a recent study, we showed that obese subjects present subtle impairments of intestinal barrier function, which were exacerbated after lipid challenge; this feature correlated with systemic and intestinal inflammation [6]. Therefore, the loss of intestinal barrier integrity is probably part of the mechanisms driving subclinical chronic inflammation.

Studies on rodents under long-term high-fat diet (HFD) have also highlighted the role of lipids in endotoxemia, but only a few have analyzed the effect of HFD on intestinal barrier integrity (for recent reviews, [5, 7]). Decreased mRNA levels of the tight junction proteins ZO-1 and occludin were observed in mouse intestine after 4 weeks of HFD [8]. Gulhane et al [9] showed that, in mice, prolonged HFD leads to increased colonic inflammation, which is associated with endotoxemia and decreased expression of the tight junction protein claudin-1 in this tissue. Some have reported that the HFD composition can influence microbiota changes, endotoxemia, and the immune response. Laugerette et al [10] compared the effects of 8-week diets enriched with different oils in mice, and showed that a palm oil–enriched diet results in the most active transport of LPS to the tissues and the highest plasma level of the proinflammatory interleukin-6 (IL-6). More recently, Lam et al [11] showed that mice fed for 8 weeks with HFD enriched with saturated fatty acids or *n*-6 polyunsaturated fatty acids displayed similar weight gain and adiposity, but only mice fed with saturated HFD exhibited increased paracellular permeability to ions, as evaluated by decreased transepithelial

electrical resistance (TEER) and macrophage infiltration in the colon. As one of the main saturated fatty acids in the human diet, palmitic acid might exert an important effect on gut permeability and inflammation, and should therefore be further investigated.

Several studies have suggested that the effects of HFD on intestinal permeability occur before the onset of obesity. Increased albumin in the feces, reflecting higher intestinal permeability, was observed as early as after 1 day of HFD, and passage of fluorescein isothiocyanate (FITC)-dextran molecules through the intestinal epithelium was increased after 7 days [12]. Moreover, studies on lean humans or on rodents under chow diet showed that a single lipid meal would lead to a moderate and transient increase in endotoxemia [13-15] and increased plasma IL-6 level [13]. In these latter studies, neither the importance of fatty acid composition of the meal (especially the effects of palmitic acid) nor the intestinal epithelial barrier integrity was documented. Nevertheless, these results suggest that an acute supply of lipids is sufficient to provoke transient alteration of the intestinal epithelial barrier.

We may hypothesize that repeated lipid supply can amplify or maintain intestinal epithelial barrier defect, which in turn could initiate low-grade inflammation or contribute to its maintenance. Here, we explored the impact of single or repeated supply of palm oil and palmitic acid on intestinal epithelial barrier integrity and its consequence on the expression of intestinal genes involved in the inflammatory response. Mechanistic investigations were conducted on endoplasmic reticulum (ER) stress and ceramide synthesis.

2. Materials and methods

2.1 Treatments, colitis induction and assessment, and intestinal permeability in mice

Three-month-old male C57BL/6J mice (Janvier Labs, Le Genest-Saint-Isle, France) were fed *ad libitum* a standard chow diet (A04, SAFE, Augy, France). The mice were kept on an artificial 12-h light–dark cycle with lights on 07:00 h. The mice were gavaged with palm oil (Sigma-Aldrich, Saint Quentin-Fallavier, France) whose fatty acid composition is rich in saturated palmitic acid (about 45%) and unsaturated oleic acid (about 35%). The mice were gavaged with 0.2 ml palm oil for one or five consecutive days at 18:00 h, i.e., just before the feeding period. Mice that received the lipid loads had 20% reduced food consumption, but the calorie intake was preserved (control mice and palm oil

treated–mice, 9 kcal/mouse/24 h and 8.8 kcal/mouse/24 h, respectively). On the last day of the experiment, the mice were successively gavaged at 9:00 h with 0.2 ml palm oil and 0.2 ml 4 kDa FITC-dextran (Sigma-Aldrich) solution (in water, 0.5 mg/g per mouse). The mice were anesthetized and then euthanized 1 h after the last gavage. Blood, the small intestine, and colon were then collected. The duodenum was removed and the rest of the small intestine was divided into two equal parts referred to here as the jejunum and ileum. For *in vivo* measurement of intestinal permeability, plasma FITC-dextran concentrations were determined by fluorometry (FLUOstar Omega; BMG Labtech, Champigny-sur-Marne, France). Colitis was induced in mice by 5 days of 3.5% dextran sodium sulfate (DSS, MP Biomedicals, Illkirch-Graffenstaden, France) in drinking water, followed by a 3-day DSS-free recovery period. All experiments involving mice were approved by the French Minister of Education and Research and by Animal Care and Use Committee N°5 (agreement number: APAFIS#2710-201510301447819).

2.2 Fecal bacterial species analysis

Mice received one gavage of 0.2 ml palm oil or water each day for four consecutive days. Fresh feces were collected 16 h after the last gavage and immediately stored at -80°C until analyzed. DNA was extracted from 100 mg feces, obtained from fecal pellets pooled from 1–3 mice, as previously described [16]. Table 1 describes the primers used for the group- and species-specific 16S rRNA targeting. PCR was performed using the Applied Biosystems StepOnePlus Real-Time PCR System (Thermo Fisher Scientific, Illkirch-Graffenstaden, France). Bacterial count in the fecal samples was determined using DNA extracted from cultured bacterial strains (Table 1) and analyzed as described previously [16]. The abundance of segmented filamentous bacteria and *Akkermansia muciniphila* was determined by relative quantification to DNA extracted from the feces of untreated mice

2.3 Cell culture and cell treatments

The Caco-2/TC7 cell line is a clonal population of human colon carcinoma–derived Caco-2 cells, which reproduce, to a high degree, most of the morphological and functional characteristics of enterocytes [17]. The cells were checked for the absence of mycoplasma contamination. In all

experiments, the cells were cultured on 6-well Transwell® filters (Thermo Fisher Scientific) for 3 weeks to obtain fully differentiated enterocyte-like cells as previously described [18, 19].

Palmitic acid or oleic acid (Sigma-Aldrich) was supplied as complex micelles to mimic their physiological form in the intestinal lumen *in vivo*. Complex micelles (2 mM sodium taurocholate, 0.6 mM oleic acid or 0.6 mM palmitic acid, 0.2 mM lysophosphatidylcholine, 0.05 mM cholesterol, 0.2 mM monoacylglycerol) were prepared in serum-free medium as previously described [19, 20] and added to the upper compartment. In some experiments, 0.3 mM or 0.1 mM palmitic acid was used instead. During epithelium integrity analysis, the micelles were removed and replaced with fresh apical medium. The release of the cytoplasmic enzyme lactate dehydrogenase (LDH) in the medium, used as a toxicity test, remained at <1% of total LDH activity of the cell lysate when palmitic or oleic acid was added to the cultured cells. In some experiments, the cells were treated with 4.5 mM EGTA (Sigma-Aldrich), which was added to the upper compartment, or with 2 mM dithiothreitol (DTT, Sigma-Aldrich), 20 mM L-cycloserine (Sigma-Aldrich), or 100 μM C_2-ceramide (Cayman Chemical, Montigny-le-Bretonneux, France) added to both the upper and lower compartments. C_2-ceramide was dissolved in 0.5% ethanol as previously described [21]. The duration of treatments is indicated in the figure legends.

2.4 Permeability measurements in Caco-2/TC7 cells

To assess paracellular permeability, 1mg/ml of 4 kDa FITC-dextran (TdB Consultancy AB, Uppsala, Sweden) was added to the apical medium on the last day of treatment. Samples of basal medium were collected after 4h, and fluorescence was determined with a microplate fluorometer (FLUOstar Omega; BMG Labtech). Transepithelial electrical resistance, which is inversely proportional to the permeability to small ions, was measured before and after treatment using a volt-ohm meter (Millipore, Guyancourt, France).

2.5 Total RNA extraction and reverse transcription (RT)-PCR

Total RNA from Caco-2/TC7 cells and from the intestinal segments was extracted with TRI Reagent (Molecular Research Center, Cincinnati, OH, USA) according to the manufacturer's instructions. RT

was performed with 1 μg RNA using a high-capacity complementary DNA (cDNA) reverse transcriptase kit (Applied Biosystem, Thermo Fisher Scientific). Semi-quantitative real-time PCR was performed with the Mx3000P Stratagene system using SYBR Green (Agilent, Les Ulis, France) according to the manufacturer's procedures. Table 2 lists the human and mouse primer sequences used. The primer sequences for the specific quantification of the spliced *XBP1* mRNA have been described previously [22].

2.6 Cytokine content and secretion

IL-8 and IL-1β protein levels were quantified by enzyme-linked immunosorbent assay (ELISA) using R&D System kits (Lille, France). For cytokine quantification in mouse intestine, whole intestinal segments were homogenized in phosphate-buffered saline (PBS) buffer using a FastPrep® instrument (MP Biomedicals), sonicated (Bioruptor®, Diagenode, Liège, Belgium), and centrifuged at 10,000 *g* for 10 min at 4°C. The supernatant (100 μg protein) was used for ELISA. For Caco-2/TC7 cell experiments, 0.2 ml basal medium was used for the ELISA.

2.7 Immunofluorescence analysis of junctional proteins

Immunofluorescence analyses were performed as previously described [23]. Briefly, Caco-2/TC7 cells were fixed and permeabilized by 5-min incubation in methanol at −20°C. Jejunum cryosections were fixed for 30 min in 4% paraformaldehyde at 4°C, and permeabilized for 30 min in 0.1% Triton X-100 at 4°C. For immunostaining of mouse jejunum cryosections, we used primary antibodies against tricellulin (1:10; Tric2469; kindly provided by Dr. Furuse [24, 25]), ZO-1 (1:200; 617300; Thermo Fisher Scientific), occludin (1:10; Moc-37; kindly provided by Dr Furuse [26]) and for E-cadherin (1:500; ECCD2 M108; Takara Bio Europe, Saint-Germain-en-Laye, France). For Caco-2/TC7 cell immunostaining, we used primary antibodies against tricellulin (1:200; MARVELD2 700191; Thermo Fisher Scientific), ZO-1 (1:200; ZO1-1A12; 33-9100 Thermo Fisher Scientific), occludin (1:200; 71-1500; Thermo Fisher Scientific), and E-cadherin (1:500; ECCD2 M108; Takara Bio Europe). Alexa 488- and Alexa 546–conjugated anti–immunoglobulin G were used as secondary antibodies (1:400;

Molecular Probes, Life Technologies, Saint-Aubin, France). The nuclei were stained with 4′-6-diamidino-2-phenylindole (DAPI) to assess the monolayer integrity. The cells were examined by microscopy using an Axio Imager 2 microscope equipped with Apotome.2, allowing optical sectioning (Zeiss, Oberkochen, Germany). Images were acquired by ZEN 2011® software (Zeiss) and analyzed in ImageJ 1.46c (https://imagej.nih.gov/ij/index.html).

2.8 *Western blotting*

Caco-2/TC7 cells were lysed as previously described [19]. Protein levels were detected in cell lysates using a Wes™ capillary electrophoresis system (ProteinSimple, San José, CA, USA) according to the manufacturer's instructions. Reconstituted images and quantification were performed using Compass software for Simple Western (ProteinSimple). The primary antibodies were rabbit anti-tricellulin (1:2000; MARVELD2 700191; Thermo Fisher Scientific), rabbit anti–ZO-1 (1:200; ZO1-1A12; 33-9100; Thermo Fisher Scientific), rabbit anti-occludin (1:25; 71-1500; Thermo Fisher Scientific), and rabbit anti–E-cadherin (1:1000; clone 36, 610181; BD Biosciences, Rungis, France). The secondary antibodies and reagents were provided in the separation and detection module kits (ProteinSimple). Junctional protein levels were normalized to Hsc70 (1:100; sc7298 Santa Cruz, CliniSciences Nanterre, France) or actin (1:1000; NB600-532SS Novus Biologicals, Bio-techne Ltd. Lille, France).

2.9 Statistical analysis

Results are expressed as the mean ± SEM. Statistical analyses were performed using GraphPad Prism 6.0 (GraphPad Software, La Jolla, CA, USA). Student's *t*-test was used for two-group comparisons. Multiple groups were compared using one-way analysis of variance (ANOVA). A p-value < 0.05 was considered significant.

3. Results

3.1 Palm oil gavage increased intestinal permeability, disrupted cell–cell junctions, and modified the expression of genes involved in inflammation in mice

We analyzed the effects of palm oil on intestinal barrier integrity in mice by measuring the intestinal permeability to 4 kDa FITC-dextran. We compared the effects of a single gavage of palm oil to daily gavages for five consecutive days. We calculated that a lipid gavage of 180 mg represents, in one intake, the daily lipid consumption (210 mg) of a mouse fed control diet containing 8% w/w fat. DSS-treated mice were used as a model of chemically induced barrier defect (for review, [27]). As previously described [28], DSS induced a 2-fold increase in intestinal permeability as compared to the control group ($p = 0.0008$) (Fig. 1A). The permeability to 4-kDa molecules after palm oil gavage was increased in the same range as in the positive control (DSS). Mice that received one palm oil gavage had higher intestinal permeability ($p < 0.0001$) than the control group. Surprisingly, no further increase was observed following multiple gavages.

As an efficient epithelial barrier is dependent on cell–cell junction integrity, we performed immunofluorescence analysis of the jejunum to determine the localization of the tight junction proteins (ZO-1, occludin, tricellulin) and the adherens junction protein E-cadherin. One palm oil gavage resulted in reduced occludin and tricellulin labeling at the apico-lateral membranes. ZO-1 labeling was more diffuse, while E-cadherin was not affected (Fig. 1B). Five consecutive palm oil gavages disrupted the distribution of all these proteins. In addition to the reduced occludin and tricellulin labeling, we observed a shift of E-cadherin and ZO-1 labeling toward the basal region of the lateral membrane (Fig. 1B, red arrows). Decreased occludin mRNA levels were observed after one and five palm oil gavages (Fig. 1C) while the mRNA levels of the other junction proteins remained unchanged (data not shown).

We analyzed the expression of several genes linked to inflammation in the intestine (Fig. 2). The protein level of the proinflammatory IL-1β tended to increase ($p = 0.053$) in the colon of mice that received one palm oil gavage; a 2.4-fold increase ($p = 0.0027$) was observed after five gavages (Fig. 2A). *Gata3* is known as a master gene controlling the functions of T cells and innate lymphoid cells [29, 30]. When compared to control mice, *Gata3* mRNA levels in the jejunum were decreased in the DSS-treated mice ($p = 0.0003$) or after five palm oil gavages ($p = 0.0024$), but not after one palm oil gavage (Fig. 2B). This suggests that the repeated palm oil gavages altered the immune response in the intestine. *Reg3g* encodes a major antimicrobial peptide involved in host defense against bacterial

invasion [31, 32]. One palm oil gavage increased *Reg3g* mRNA levels ($p = 0.0118$) in the ileum as compared to the control group (Fig. 2C). However, *Reg3g* mRNA levels were unchanged in the ileum of mice that received repeated gavages and in DSS-treated mice. This suggests that one palm oil gavage engaged the antimicrobial host defense, which would be lost or less effective after repeated palm oil gavages. We may hypothesize that repeated palm oil treatment impairs the antimicrobial host defense and could participate in intestinal barrier defects. This result also suggests that changes in microbiota composition could occur after palm oil treatment.

Altogether, we show *in vivo* in mice that short-term treatment with palm oil is sufficient to provoke the mislocalization of key junctional proteins to increase intestinal permeability and to modify the expression of several genes involved in the immune response in the intestine.

3.2 Palm oil gavages modified fecal bacterial species in mice

There are major changes in the relative abundance of bacterial species during high-fat feeding (for review, [33]). Palm oil might affect bacterial abundance via bacterial growth or modification of the genes involved in the antimicrobial response (e.g., *Reg3g*) as previously observed after long-term HFD [34]. We measured the abundance of selected fecal bacteria after four palm oil gavages. We found significantly decreased *Clostridium leptum* (Fig. 3A, $p=0.0273$), *Akkermansia muciniphila* (Fig. 3B, $p=0.0274$) and segmented filamentous bacteria (Fig. 3C, $p=0.0133$) abundance after four palm oil gavages, while *Bacteroides* sp. abundance was increased (Fig. 3D, $p=0.0230$). The abundance of *Lactobacillus* sp. (Fig. 3E) and *Clostridium coccoides* (Fig. 3F), and total bacteria count (Fig. 3G), were unaffected. These results indicate that four palm oil gavages can modify gut bacterial species composition.

3.3 Palmitic acid disrupts permeability and cytokine expression in human intestinal epithelial cells

To characterize the impact of lipids on the intestinal epithelial compartment, we investigated the effects of palmitic and oleic acid, two major fatty acids present in palm oil. We analyzed the effects of the two fatty acids, delivered as complex micelles, on the paracellular permeability of a human Caco-2/TC7 cell monolayer. The cells were incubated for 24 h or daily for four consecutive

days with either palmitic or oleic acid micelles. The positive control was 24-h treatment with 4.5 mM EGTA, a calcium chelator known to increase epithelial permeability [35, 36]. As expected, EGTA increased the permeability of the Caco-2/TC7 cell monolayer to 4 kDa FITC-dextran ($p < 0.0001$) (Fig. 4A) and to ions (decreased TEER, $p < 0.0001$) (Fig. 4C). Interestingly, 1-day treatment with palmitic acid provoked significantly increased 4 kDa FITC-dextran flux (Fig. 4A) without significant changes in permeability as assessed by TEER (Fig. 4D). A repeated supply of palmitic acid for 4 days markedly enhanced the permeability of the monolayer to 4 kDa FITC-dextran ($p = 0.0152$). TEER was decreased as early as the first 48 h of treatment ($p = 0.038$). These effects were not observed when oleic acid was used. A dose–response effect of palmitic acid concentration was observed for 4 kDa FITC-dextran flux (Fig. 4B) and TEER (Fig. 4E).

We performed immunofluorescence analysis of the localization of ZO-1, occludin, tricellulin, and E-cadherin in cells treated with palmitic acid or oleic acid micelles (Fig. 5A). In cells incubated for 24 h with palmitic acid, all junctional proteins had decreased fluorescence intensity, without modification of their localization at cell–cell contacts. However, repeated supply of palmitic acid micelles over 4 days provoked the internalization of E-cadherin, ZO-1, and occludin, and the loss of tricellulin at the tricellular junctions. In accordance with the absence of effects on paracellular permeability, the oleic acid micelles did not alter the junctional protein distribution. The total cell lysates showed decreased E-cadherin, occludin, and tricellulin protein levels, but not ZO-1, in cells treated for 4 days with palmitic acid (Fig. 5B–F). No modification of junctional protein levels was observed in total cell lysates from cells treated for 24 h with palmitic or oleic acid (data not shown). Occludin mRNA levels were decreased after 4-day palmitic acid treatment (Fig. 5G) but the mRNA levels of the other junctional proteins were unchanged (data not shown). Altogether, these results showed that 4-day palmitic acid treatment impairs both the expression of junctional proteins and their localization at cell-cell contacts.

Intestinal epithelial cells can produce several cytokines [37, 38] among which the *CXCL8* (IL-8), *TGFB1* (transforming growth factor β1), and *IL1B* genes are particularly well expressed in Caco-2/TC7 cells. We determined whether palmitic acid could induce the production of these cytokines. Cells were treated for 24 h or 4 days with palmitic acid or oleic acid micelles (Fig. 6). Palmitic acid

increased IL-8 expression as early as after 24-h treatment ($p = 0.0214$; Fig. 6A) and increased its secretion in basal medium after 4-day treatment (Fig. 6B), while oleic acid did not exert any effect. A dose-dependent increase in *IL8* mRNA expression (Fig. 6E) and a trend for increased IL-8 secretion (Fig. 6G) were observed upon palmitic acid treatment. *TGFB1* mRNA levels ($p = 0.0022$) were slightly decreased after repeated supply of palmitic acid (Fig. 6C), whereas oleic acid did not alter *TGFB1* expression. A lower concentration of palmitic acid (0.1 or 0.3 mM instead of 0.6 mM) was not sufficient to modulate *TGFB1* expression (Fig. 6F). Neither oleic acid nor palmitic acid modified *IL1B* mRNA levels, regardless of treatment duration (Fig. 6D). Interestingly, EGTA increased *IL8* ($p < 0.0001$) and *IL1B* mRNA levels ($p < 0.0001$) and IL-8 secretion ($p = 0.0042$), indicating that the destabilization of cell–cell junctions was sufficient for inducing cytokine production

We next determined whether the effects of palmitic acid were reversible after its removal from the culture medium (Fig. 7). Cells were treated daily for 4 days with palmitic acid micelles, and then cultured in control medium for one or two more days. We observed a time-dependent decrease of 4 kDa FITC-dextran passage through the monolayer after the removal of palmitic acid. However, 2 days after micelle removal, the paracellular permeability of the monolayer remained 3.5-fold higher than that of untreated cells (Fig. 7A, $p = 0.0008$). Removing palmitic acid did not restore the basal level of TEER either, which remained 10–15% lower than that of the control cells (Fig. 7B, $p = 0.007$). Immunofluorescence analyses of the junctional proteins were performed after 4-day palmitic acid treatment and at 1 and 2 days after its removal (Fig. 7C). Gradually improved occludin and tricellulin distribution over time was observed after palmitic acid removal. E-cadherin and ZO-1 distribution remained largely altered even 2 days after the cells had been returned to the control medium. Western blotting showed that tricellulin (Fig. 7D), and E-cadherin and ZO-1 (data not shown) protein amounts recovered 2 days after palmitic acid removal. While occludin mRNA levels returned to control values 2 days after palmitic acid removal (Fig. 7E), the occludin protein amount remained lower than that in the control cells (Fig. 7D). Moreover, the effects of palmitic acid on *IL8* (Fig. 7F) and *TGFB1* (Fig. 7G) mRNA levels were abolished at 2 days and 1 day, respectively, after its removal from the culture medium. Altogether, these results show that the effects of palmitic acid are attenuated slowly after the arrest of treatment.

3.4 Palmitic acid induced moderate ER stress

We analyzed the molecular mechanisms involved in the effects of palmitic acid on barrier integrity and cytokine production in Caco-2/TC7 cells. Palmitic acid is known as a more potent ER stress inducer than oleic acid [39-42]. Moreover, the induction of ER stress by various stimuli, including fatty acids, can increase cytokine expression in several cell types [43, 44] and may trigger epithelial barrier dysfunction (for review, [45]). We therefore wanted to determine whether the observed effects of palmitic acid were due to the induction of ER stress. Accordingly, Caco-2/TC7 cells were treated for 24 h or daily on four consecutive days with palmitic acid or oleic acid micelles. The cells were then treated with 2 mM DTT, a known inducer of ER stress [46, 47]. As expected, DTT increased paracellular permeability (Fig. 8A) and *IL8* mRNA levels (Fig. 8B). DTT induction of ER stress was assessed through the increased expression of *GRP78*/*HSPA5*, *GADD153*/*DDIT3*, and the spliced form of *XBP1* (Fig. 8C–E), three gene markers of unfolded protein response. Oleic acid provoked moderate induction of *GRP78/HSPA5* expression, which was detected only after 24-h treatment ($p = 0.0085$) but not after 4 days (Fig. 8C), while *GADD153/DDIT3* and spliced *XBP1* mRNA levels were unchanged (Fig. 8D–E). Palmitic acid increased the expression of these three gene markers of ER stress, but to a limited extent as compared to DTT. This effect was mainly observed after 24-h treatment (Fig. 8C–E). As both palmitic and oleic acid induce moderate ER stress, while only palmitic acid alters epithelial barrier integrity and increases IL-8 expression, we concluded that ER stress cannot explain the specific effects of palmitic acid. We speculate that other molecular mechanisms may be involved in the deleterious effects of palmitic acid.

3.5 Ceramides mediated the deleterious effects of palmitic acid on epithelial barrier function and immune response

Palmitic acid, but not oleic acid, is a precursor of *de novo* ceramide synthesis (for review, [48]), which contributes not only to membrane structure but also to signaling and metabolic dysfunctions in various cell types, including Caco-2/TC7 cells [21, 49]. Accordingly, we wanted to determine whether ceramides could provoke epithelial barrier damage and induce cytokine production.

Caco-2/TC7 cells were treated with C_2-ceramide, a short chain, cell-permeating, biologically active ceramide analogue. The 24-h C_2-ceramide treatment markedly increased paracellular permeability ($p < 0.0001$) (Fig. 9A) and decreased TEER ($p < 0.0001$) (Fig. 9B). These effects were associated with decreased expression of all junctional proteins (Fig. 9C). Immunofluorescence analysis showed altered ZO-1, occludin, tricellulin, and E-cadherin localization at the cell–cell contacts (Fig. 9D). C_2-ceramide increased IL-8 expression and secretion ($p = 0.0201$, Fig. 9E, F), decreased *TGFB1* mRNA levels ($p = 0.038$, Fig. 9G), and had no effect on *IL1B* mRNA levels (Fig. 9H). For all these parameters, no effect was observed for ethanol, used as the vehicle for C_2-ceramide. Altogether, these results show that C_2-ceramide induces effects similar to that of palmitic acid on intestinal epithelial barrier integrity and cytokine production.

We determined whether inhibiting *de novo* ceramide synthesis could attenuate the deleterious effects of palmitic acid. Caco-2/TC7 cells were treated with L-cycloserine, an irreversible inhibitor of serine palmitoyl transferase, the first enzyme of *de novo* ceramide synthesis [50, 51]. L-cycloserine did not modify the paracellular permeability of the Caco-2/TC7 cell monolayer at the basal state or in the presence of palmitic acid micelles (Fig. 10A). However, it abolished the palmitic acid-dependent increase in *IL-8* mRNA levels (Fig. 10B). These results suggest that, in human enterocytes i.e., Caco-2/TC7 cells; the effects of palmitic acid on cytokine expression are dependent on *de novo* ceramide synthesis.

4. Discussion

Multiple studies on rodents with obesity induced by long-term HFD have linked increased gut permeability to inflammation and metabolic alterations [7, 8]. It has been proposed that endotoxemia, i.e., the passage of bacterial LPS into the systemic circulation, is a consequence of an altered intestinal barrier and is the main contributor of the low-grade inflammation triggered by diet-induced obesity [3]. However, in such animal models of diet-induced obesity, and in established obesity in humans, the initiating events remain unknown. Moreover in such situations, it is difficult to establish the sequence of events linking hyperpermeability to inflammation as the two processes are highly interconnected. Here, we show that short-term feeding with palm oil is sufficient to disrupt the intestinal barrier

integrity in mice. We observed that, in normal mice, a single intake of palm oil provoked increased intestinal permeability, accompanied by the loss of several tight junction proteins at the cell–cell contacts. This indicates that intestinal hyperpermeability is an immediate response to palm oil (Fig. 11). This rapid intestinal barrier defect is in accordance with the increased albumin fecal content, a marker of intestinal permeability, previously reported in mice 1 day after beginning a HFD [12]. Increased expression of the gene encoding the antimicrobial peptide REG3γ, i.e., *Reg3g*, as early as after one palm oil gavage suggests that the intestine has already engaged the mucosal defense (Fig. 11). No modulation of genes involved in the intestinal immune response was detected after a single bolus. Importantly, our results, obtained from a human enterocyte model, demonstrate that palmitic acid can exert its deleterious effects directly on the epithelial compartment independently of immune cells and microbiota. Palmitic acid disrupted cell–cell junctions in Caco-2/TC7 cells, resulting in increased paracellular permeability. In association with these effects on the epithelial barrier, palmitic acid increased the expression and secretion of the proinflammatory cytokine IL-8, suggesting that the initiation of an inflammatory response may occur in the epithelial compartment (Fig. 11).

Our results identify the intestinal epithelial compartment as an early target of the deleterious effects exerted by dietary lipids. In mice, markedly increased permeability is detected before the modulation of genes involved in the intestinal immune response, suggesting that the disruption of the intestinal barrier is the primary event. However, in human Caco-2/TC7 enterocytes, both increased permeability and IL-8 expression were observed after 24-h palmitic acid treatment, suggesting that, in human epithelial cells, hyperpermeability and the initiation of the immune response occur concomitantly. IL-8 is produced by many cell types, including intestinal epithelial cells, and participates in the acute-phase response of inflammation [52]. In the intestine, IL-8 is involved in recruiting neutrophils in the mucosa, where they participate in the host defense against bacterial invasion. Interestingly, contrary to humans, mice do not express IL-8 [53]. It remains to determine whether the hierarchy of events linking hyperpermeability and inflammation differs between humans and mice

When the palm oil gavages were repeated, additional gut alterations were observed together with the increased epithelial permeability (Fig. 11). Indeed, IL-1β was increased in the colon, and

Gata3 mRNA levels were decreased in the proximal intestine. *Gata3* is a key transcription factor involved in the differentiation and maturation of the innate lymphoid cells controlling the expression of both proinflammatory and anti-inflammatory cytokines [30]. A link between *Gata3* activity and visceral fat inflammation during obesity was recently reported [54]. However, its exact role in intestinal inflammation remains to be characterized. Interestingly, the increased *Reg3g* mRNA levels observed after one palm oil gavage were not observed after repeated gavages. As *Reg3g* is involved in the host defense against bacteria, this suggests that saturated fat overload results in a decreased efficiency of the intestinal defense response. The observation that the effects of palmitic acid in Caco-2/TC7 cells were not reversed as rapidly as they occurred is consistent with our original hypothesis that repetition of lipid intake could maintain an intestinal epithelial barrier defect and initiate low-grade inflammation. Cytokines produced by both the epithelial and immune cells could further contribute to amplifying hyperpermeability. Indeed, both IL-1β and IL-8 disrupt the tight junction proteins [55, 56]. Increased IL-1β expression in the intestine is frequently reported in HFD models and in human obesity (for review, [57]). It is not known whether these cytokines participated in the alteration of tight junctions in our models (Fig. 11). Altogether, these results show that palm oil or palmitic acid initiates an imbalanced immune response favoring a proinflammatory profile. We hypothesize that cytokines produced by epithelial cells in response to palm oil or palmitic acid may also activate the intestinal immune cells, thereby creating a vicious cycle maintaining intestinal inflammation. It has not been determined whether this initiation of intestinal inflammation by lipids can eventually lead to systemic inflammation.

In association with changes in immune-related gene expression and intestinal barrier defects, we observed that repeated palm oil gavages provoked changes in microbiota composition (Fig. 11). We studied some bacteria species previously reported as modified by HFD or obesity, and observed decreased fecal abundance of *C. leptum*, *A. muciniphila*, and segmented filamentous bacteria in palm oil–treated mice as compared to the control. These bacteria species exert a protective role against pathogen proliferation and contribute to host defense by promoting immune cell maturation [58]. Their decreased abundances were related to the inflammatory status of the tissue. The anti-inflammatory properties of *A. muciniphila* have gained attention and highlight its importance as a

therapeutic target for treating intestinal inflammation [59]. In particular, gut *A. muciniphila* abundance is reduced in human obesity [60, 61] and in HFD-induced obesity in mice [62]. The decreased abundance of segmented filamentous bacteria observed after palm oil gavages is in accordance with their reduction in mice on long-term HFD [63], but its role in inflammation remains uncertain [64]. We observed increased *Bacteroides* sp. in palm oil–treated mice, congruent with several reports showing increased abundance of this species associated with the consumption of HFD rich in saturated fatty acids [65-68]. We may conclude that four gavages with palm oil are sufficient for promoting changes in microbiota composition corresponding to the changes reported in obesity induced by HFD and relevant to gut inflammation.

Studies of the molecular mechanisms involved in the deleterious effects of palmitic acid on intestinal epithelial cells have revealed the contribution of *de novo* synthesis of ceramides. In established obesity, increased circulating saturated fatty acids and inflammatory signals promote ceramide synthesis [69]. Here, we observed that C2-ceramide acted on three parameters: increase in intestinal epithelial permeability, mislocalization of junctional proteins and modification of cytokine expression. Interestingly, intestinal barrier defect was recently shown to be associated with elevated C16-ceramide levels [70] and with increased ceramide content induced by the addition of sphingomyelinase [71]. Ceramides can increase permeability through their property of disrupting membrane raft domains [72-74], where several junctional proteins are localized [75, 76]. Ceramides may also alter membrane integrity by their channel-formation capacity [77]. Nevertheless, we observed that inhibiting *de novo* ceramide synthesis reduced pro-inflammatory cytokine expression but failed to restore cell monolayer permeability, suggesting a role of *de novo* ceramide synthesis limited to the inflammatory process. Very few studies have analyzed the direct effect of ceramides on cytokine expression; however, C_2-ceramide induction of IL-6 has been reported in human fibroblasts [78] and human astrocytoma cells [79]. We show that inhibiting *de novo* ceramide synthesis prevented increased IL-8 secretion in palmitic acid–treated cells. Therefore, palmitic acid engages multiple mechanisms, including ceramide pathways, to exert its deleterious effects on intestinal permeability and inflammation.

Recent advances have suggested that fatty acids may act by binding to membrane receptors (e.g., TLRs and G protein–coupled receptors) or nuclear receptors (e.g., PPARs, LXR, or FXR) and the subsequent rapid activation of signaling cascades (for review, [80]). Here, our study demonstrates the specific effect of palmitic acid, as oleic acid had no effect on intestinal barrier integrity and cytokine expression. However, several fatty acids, such as short- and medium-chain fatty acids, modulate intestinal barrier integrity (for review, [80]). Interestingly, we observed in the Caco-2/TC7 cells that very short treatment (4 h) with oleic acid in the form of mixed micelles might disrupt tricellulin distribution and increase intestinal permeability [6]. Altogether, these data underline the differential effects of fatty acids according to their nature and length of exposure on intestinal barrier integrity. Altogether, these data underlie the differential effects of fatty acids, based on their nature and duration of exposure, on intestinal barrier integrity. Fritsche [81] reviewed the beneficial or deleterious effects of fatty acids on the intestinal barrier and inflammation. Interestingly, the presence of oleic acid can counteract or diminish the deleterious effect of palmitic acid on cellular functions [82]. Other lipids or nutrients contribute to barrier dysfunctions [83].

In healthy humans, meals are constituted of mixed nutrients, intestinal barrier integrity is maintained, and post-prandial inflammation is limited. Nevertheless, in pathological conditions, there might be chronicization of the alteration of barrier functions. Indeed, we have previously observed that obese subjects present only subtle intestinal barrier defects that can be revealed after lipid load [6], and hyperglycemia was recently described as disrupting the gut barrier [84]. Therefore, excess nutrients in the pathological context might further aggravate barrier dysfunctions, probably by exceeding the regulatory capacities of the gut. Further studies are needed to identify the other contributors of metabolic-associated gut barrier defects.

In conclusion, our results show that limited repeated supply of saturated fatty acids, and particularly palmitic acid, are sufficient for inducing intestinal barrier defect, initiating the intestinal inflammatory response, and altering microbiota composition. These gut alterations, occurring before the onset of diet-induced obesity, may therefore represent the initiating events of the low-grade inflammation observed once the disease is established.

5. Acknowledgements

S.G. received a doctoral fellowship from Sorbonne Université (formerly Université Pierre et Marie Curie), Paris, France. B.G.P. is recipient of doctoral fellowship CNPq 207303/2014-2 from the Science Without Border program of the Brazilian government. We thank all the staff in charge of animal housing and care at the animal core facility of the Centre d'Explorations Fonctionnelles at the Centre de Recherche des Cordeliers, Paris, France. We thank Dr Furuse (National Institute for Physiological Sciences, Okazaki, Japan) for kindly providing us antibodies directed against occludin and tricellulin.

6. Conflict of interest

No conflict of interest declared.

7. Authors contributions

S.G., B.G.P., S.T. and V.C. designed and conducted the experiments and analyzed the data. E.Q., L.B., P.S. managed the microbiota analysis. S.G. and V.C. wrote the paper. B.G.P., S.T., P.S., E.Q. and A.L. revised the manuscript. All authors reviewed the results and approved the final version of the manuscript.

8. References

[1] S.S. Pereira, J.I. Alvarez-Leite, Low-Grade Inflammation, Obesity, and Diabetes, Curr Obes Rep, 3 (2014) 422-431.
[2] M. Monteiro-Sepulveda, S. Touch, C. Mendes-Sa, S. Andre, C. Poitou, O. Allatif, A. Cotillard, H. Fohrer-Ting, E.L. Hubert, R. Remark, L. Genser, J. Tordjman, K. Garbin, C. Osinski, C. Sautes-Fridman, A. Leturque, K. Clement, E. Brot-Laroche, Jejunal T Cell Inflammation in Human Obesity Correlates with Decreased Enterocyte Insulin Signaling, Cell metabolism, 22 (2015) 113-124.
[3] P.D. Cani, J. Amar, M.A. Iglesias, M. Poggi, C. Knauf, D. Bastelica, A.M. Neyrinck, F. Fava, K.M. Tuohy, C. Chabo, A. Waget, E. Delmee, B. Cousin, T. Sulpice, B. Chamontin, J. Ferrieres, J.F. Tanti, G.R. Gibson, L. Casteilla, N.M. Delzenne, M.C. Alessi, R. Burcelin, Metabolic endotoxemia initiates obesity and insulin resistance, Diabetes, 56 (2007) 1761-1772.
[4] A.L. Neves, J. Coelho, L. Couto, A. Leite-Moreira, R. Roncon-Albuquerque, Jr., Metabolic endotoxemia: a molecular link between obesity and cardiovascular risk, Journal of molecular endocrinology, 51 (2013) R51-64.
[5] N.E. Boutagy, R.P. McMillan, M.I. Frisard, M.W. Hulver, Metabolic endotoxemia with obesity: Is it real and is it relevant?, Biochimie, 124 (2016) 11-20.
[6] L. Genser, D. Aguanno, H.A. Soula, L. Dong, L. Trystram, K. Assmann, J.E. Salem, J.C. Vaillant, J.M. Oppert, F. Laugerette, M.C. Michalski, P. Wind, M. Rousset, E. Brot-Laroche, A. Leturque, K.

Clement, S. Thenet, C. Poitou, Increased jejunal permeability in human obesity is revealed by a lipid challenge and is linked to inflammation and type 2 diabetes, J Pathol, (2018).
[7] J.R. Araujo, J. Tomas, C. Brenner, P.J. Sansonetti, Impact of high-fat diet on the intestinal microbiota and small intestinal physiology before and after the onset of obesity, Biochimie, 141 (2017) 97-106.
[8] P.D. Cani, R. Bibiloni, C. Knauf, A. Waget, A.M. Neyrinck, N.M. Delzenne, R. Burcelin, Changes in gut microbiota control metabolic endotoxemia-induced inflammation in high-fat diet-induced obesity and diabetes in mice, Diabetes, 57 (2008) 1470-1481.
[9] M. Gulhane, L. Murray, R. Lourie, H. Tong, Y.H. Sheng, R. Wang, A. Kang, V. Schreiber, K.Y. Wong, G. Magor, S. Denman, J. Begun, T.H. Florin, A. Perkins, P.O. Cuiv, M.A. McGuckin, S.Z. Hasnain, High Fat Diets Induce Colonic Epithelial Cell Stress and Inflammation that is Reversed by IL-22, Sci Rep, 6 (2016) 28990.
[10] F. Laugerette, J.P. Furet, C. Debard, P. Daira, E. Loizon, A. Geloen, C.O. Soulage, C. Simonet, J. Lefils-Lacourtablaise, N. Bernoud-Hubac, J. Bodennec, N. Peretti, H. Vidal, M.C. Michalski, Oil composition of high-fat diet affects metabolic inflammation differently in connection with endotoxin receptors in mice, Am J Physiol Endocrinol Metab, 302 (2012) E374-386.
[11] Y.Y. Lam, C.W. Ha, J.M. Hoffmann, J. Oscarsson, A. Dinudom, T.J. Mather, D.I. Cook, N.H. Hunt, I.D. Caterson, A.J. Holmes, L.H. Storlien, Effects of dietary fat profile on gut permeability and microbiota and their relationships with metabolic changes in mice, Obesity (Silver Spring), 23 (2015) 1429-1439.
[12] A.M. Johnson, A. Costanzo, M.G. Gareau, A.M. Armando, O. Quehenberger, J.M. Jameson, J.M. Olefsky, High fat diet causes depletion of intestinal eosinophils associated with intestinal permeability, PloS one, 10 (2015) e0122195.
[13] F. Laugerette, C. Vors, A. Geloen, M.A. Chauvin, C. Soulage, S. Lambert-Porcheron, N. Peretti, M. Alligier, R. Burcelin, M. Laville, H. Vidal, M.C. Michalski, Emulsified lipids increase endotoxemia: possible role in early postprandial low-grade inflammation, J Nutr Biochem, 22 (2011) 53-59.
[14] S. Ghoshal, J. Witta, J. Zhong, W. de Villiers, E. Eckhardt, Chylomicrons promote intestinal absorption of lipopolysaccharides, Journal of lipid research, 50 (2009) 90-97.
[15] C. Erridge, T. Attina, C.M. Spickett, D.J. Webb, A high-fat meal induces low-grade endotoxemia: evidence of a novel mechanism of postprandial inflammation, Am J Clin Nutr, 86 (2007) 1286-1292.
[16] H. Sokol, P. Seksik, J.P. Furet, O. Firmesse, I. Nion-Larmurier, L. Beaugerie, J. Cosnes, G. Corthier, P. Marteau, J. Dore, Low counts of Faecalibacterium prausnitzii in colitis microbiota, Inflamm Bowel Dis, 15 (2009) 1183-1189.
[17] I. Chantret, A. Rodolosse, A. Barbat, E. Dussaulx, E. Brot-Laroche, A. Zweibaum, M. Rousset, Differential expression of sucrase-isomaltase in clones isolated from early and late passages of the cell line Caco-2: evidence for glucose-dependent negative regulation, Journal of cell science, 107 (Pt 1) (1994) 213-225.
[18] E. Morel, S. Ghezzal, G. Lucchi, C. Truntzer, J.P. Pais de Barros, F. Simon-Plas, S. Demignot, C. Mineo, P.W. Shaul, A. Leturque, M. Rousset, V. Carriere, Cholesterol trafficking and raft-like membrane domain composition mediate scavenger receptor class B type 1-dependent lipid sensing in intestinal epithelial cells, Biochimica et biophysica acta, 1863 (2018) 199-211.
[19] O. Beaslas, C. Cueille, F. Delers, D. Chateau, J. Chambaz, M. Rousset, V. Carriere, Sensing of dietary lipids by enterocytes: a new role for SR-BI/CLA-1, PloS one, 4 (2009) e4278.
[20] D. Chateau, T. Pauquai, F. Delers, M. Rousset, J. Chambaz, S. Demignot, Lipid micelles stimulate the secretion of triglyceride-enriched apolipoprotein B48-containing lipoproteins by Caco-2 cells, Journal of cellular physiology, 202 (2005) 767-776.
[21] T.T. Tran, B.G. Postal, S. Demignot, A. Ribeiro, C. Osinski, J.P. Pais de Barros, A. Blachnio-Zabielska, A. Leturque, M. Rousset, P. Ferre, E. Hajduch, V. Carriere, Short Term Palmitate Supply Impairs Intestinal Insulin Signaling via Ceramide Production, The Journal of biological chemistry, 291 (2016) 16328-16338.
[22] A. van Schadewijk, E.F. van't Wout, J. Stolk, P.S. Hiemstra, A quantitative method for detection of spliced X-box binding protein-1 (XBP1) mRNA as a measure of endoplasmic reticulum (ER) stress, Cell Stress Chaperones, 17 (2012) 275-279.

[23] C.S. Petit, F. Barreau, L. Besnier, P. Gandille, B. Riveau, D. Chateau, M. Roy, D. Berrebi, M. Svrcek, P. Cardot, M. Rousset, C. Clair, S. Thenet, Requirement of cellular prion protein for intestinal barrier function and mislocalization in patients with inflammatory bowel disease, Gastroenterology, 143 (2012) 122-132 e115.
[24] J. Ikenouchi, H. Sasaki, S. Tsukita, M. Furuse, S. Tsukita, Loss of occludin affects tricellular localization of tricellulin, Molecular biology of the cell, 19 (2008) 4687-4693.
[25] J. Ikenouchi, M. Furuse, K. Furuse, H. Sasaki, S. Tsukita, S. Tsukita, Tricellulin constitutes a novel barrier at tricellular contacts of epithelial cells, The Journal of cell biology, 171 (2005) 939-945.
[26] M. Saitou, Y. Ando-Akatsuka, M. Itoh, M. Furuse, J. Inazawa, K. Fujimoto, S. Tsukita, Mammalian occludin in epithelial cells: its expression and subcellular distribution, Eur J Cell Biol, 73 (1997) 222-231.
[27] D.D. Eichele, K.K. Kharbanda, Dextran sodium sulfate colitis murine model: An indispensable tool for advancing our understanding of inflammatory bowel diseases pathogenesis, World J Gastroenterol, 23 (2017) 6016-6029.
[28] Y. Yan, V. Kolachala, G. Dalmasso, H. Nguyen, H. Laroui, S.V. Sitaraman, D. Merlin, Temporal and spatial analysis of clinical and molecular parameters in dextran sodium sulfate induced colitis, PloS one, 4 (2009) e6073.
[29] J. Zhu, GATA3 Regulates the Development and Functions of Innate Lymphoid Cell Subsets at Multiple Stages, Front Immunol, 8 (2017) 1571.
[30] Y.Y. Wan, GATA3: a master of many trades in immune regulation, Trends Immunol, 35 (2014) 233-242.
[31] L. Wang, D.E. Fouts, P. Starkel, P. Hartmann, P. Chen, C. Llorente, J. DePew, K. Moncera, S.B. Ho, D.A. Brenner, L.V. Hooper, B. Schnabl, Intestinal REG3 Lectins Protect against Alcoholic Steatohepatitis by Reducing Mucosa-Associated Microbiota and Preventing Bacterial Translocation, Cell Host Microbe, 19 (2016) 227-239.
[32] L.M. Loonen, E.H. Stolte, M.T. Jaklofsky, M. Meijerink, J. Dekker, P. van Baarlen, J.M. Wells, REG3gamma-deficient mice have altered mucus distribution and increased mucosal inflammatory responses to the microbiota and enteric pathogens in the ileum, Mucosal Immunol, 7 (2014) 939-947.
[33] E.A. Murphy, K.T. Velazquez, K.M. Herbert, Influence of high-fat diet on gut microbiota: a driving force for chronic disease risk, Current opinion in clinical nutrition and metabolic care, 18 (2015) 515-520.
[34] A. Everard, V. Lazarevic, N. Gaia, M. Johansson, M. Stahlman, F. Backhed, N.M. Delzenne, J. Schrenzel, P. Francois, P.D. Cani, Microbiome of prebiotic-treated mice reveals novel targets involved in host response during obesity, ISME J, 8 (2014) 2116-2130.
[35] X. Boulenc, E. Marti, H. Joyeux, C. Roques, Y. Berger, G. Fabre, Importance of the paracellular pathway for the transport of a new bisphosphonate using the human CACO-2 monolayers model, Biochemical pharmacology, 46 (1993) 1591-1600.
[36] P. Artursson, Epithelial transport of drugs in cell culture. I: A model for studying the passive diffusion of drugs over intestinal absorptive (Caco-2) cells, Journal of pharmaceutical sciences, 79 (1990) 476-482.
[37] A.W. Stadnyk, Intestinal epithelial cells as a source of inflammatory cytokines and chemokines, Can J Gastroenterol, 16 (2002) 241-246.
[38] N. Miron, V. Cristea, Enterocytes: active cells in tolerance to food and microbial antigens in the gut, Clin Exp Immunol, 167 (2012) 405-412.
[39] V. Pardo, A. Gonzalez-Rodriguez, J. Muntane, S.C. Kozma, A.M. Valverde, Role of hepatocyte S6K1 in palmitic acid-induced endoplasmic reticulum stress, lipotoxicity, insulin resistance and in oleic acid-induced protection, Food Chem Toxicol, 80 (2015) 298-309.
[40] J. Deguil, L. Pineau, E.C. Rowland Snyder, S. Dupont, L. Beney, A. Gil, G. Frapper, T. Ferreira, Modulation of lipid-induced ER stress by fatty acid shape, Traffic, 12 (2011) 349-362.
[41] H. Danino, K. Ben-Dror, R. Birk, Exocrine pancreas ER stress is differentially induced by different fatty acids, Exp Cell Res, 339 (2015) 397-406.
[42] J.M. Caviglia, C. Gayet, T. Ota, A. Hernandez-Ono, D.M. Conlon, H. Jiang, E.A. Fisher, H.N. Ginsberg, Different fatty acids inhibit apoB100 secretion by different pathways: unique roles for ER stress, ceramide, and autophagy, Journal of lipid research, 52 (2011) 1636-1651.

[43] J.A. Willy, S.K. Young, J.L. Stevens, H.C. Masuoka, R.C. Wek, CHOP links endoplasmic reticulum stress to NF-kappaB activation in the pathogenesis of nonalcoholic steatohepatitis, Molecular biology of the cell, 26 (2015) 2190-2204.
[44] A.C. Tang, A. Saferali, G. He, A.J. Sandford, L.J. Strug, S.E. Turvey, Endoplasmic Reticulum Stress and Chemokine Production in Cystic Fibrosis Airway Cells: Regulation by STAT3 Modulation, J Infect Dis, 215 (2017) 293-302.
[45] X. Ma, Z. Dai, K. Sun, Y. Zhang, J. Chen, Y. Yang, P. Tso, G. Wu, Z. Wu, Intestinal Epithelial Cell Endoplasmic Reticulum Stress and Inflammatory Bowel Disease Pathogenesis: An Update Review, Front Immunol, 8 (2017) 1271.
[46] C.M. Oslowski, F. Urano, Measuring ER stress and the unfolded protein response using mammalian tissue culture system, Methods Enzymol, 490 (2011) 71-92.
[47] D.R. Beriault, G.H. Werstuck, Detection and quantification of endoplasmic reticulum stress in living cells using the fluorescent compound, Thioflavin T, Biochimica et biophysica acta, 1833 (2013) 2293-2301.
[48] B.M. Castro, M. Prieto, L.C. Silva, Ceramide: a simple sphingolipid with unique biophysical properties, Progress in lipid research, 54 (2014) 53-67.
[49] J.A. Chavez, S.A. Summers, A ceramide-centric view of insulin resistance, Cell metabolism, 15 (2012) 585-594.
[50] J. Lowther, B.A. Yard, K.A. Johnson, L.G. Carter, V.T. Bhat, M.C. Raman, D.J. Clarke, B. Ramakers, S.A. McMahon, J.H. Naismith, D.J. Campopiano, Inhibition of the PLP-dependent enzyme serine palmitoyltransferase by cycloserine: evidence for a novel decarboxylative mechanism of inactivation, Mol Biosyst, 6 (2010) 1682-1693.
[51] M.S. Kang, K.H. Ahn, S.K. Kim, H.J. Jeon, J.E. Ji, J.M. Choi, K.M. Jung, S.Y. Jung, D.K. Kim, Hypoxia-induced neuronal apoptosis is mediated by de novo synthesis of ceramide through activation of serine palmitoyltransferase, Cell Signal, 22 (2010) 610-618.
[52] E. Gruys, M.J. Toussaint, T.A. Niewold, S.J. Koopmans, Acute phase reaction and acute phase proteins, J Zhejiang Univ Sci B, 6 (2005) 1045-1056.
[53] H. Nomiyama, N. Osada, O. Yoshie, The evolution of mammalian chemokine genes, Cytokine Growth Factor Rev, 21 (2010) 253-262.
[54] G. Qiang, H.W. Kong, D. Fang, M. McCann, X. Yang, G. Du, M. Bluher, J. Zhu, C.W. Liew, The obesity-induced transcriptional regulator TRIP-Br2 mediates visceral fat endoplasmic reticulum stress-induced inflammation, Nat Commun, 7 (2016) 11378.
[55] R. Al-Sadi, S. Guo, D. Ye, K. Dokladny, T. Alhmoud, L. Ereifej, H.M. Said, T.Y. Ma, Mechanism of IL-1beta modulation of intestinal epithelial barrier involves p38 kinase and activating transcription factor-2 activation, J Immunol, 190 (2013) 6596-6606.
[56] H. Yu, X. Huang, Y. Ma, M. Gao, O. Wang, T. Gao, Y. Shen, X. Liu, Interleukin-8 regulates endothelial permeability by down-regulation of tight junction but not dependent on integrins induced focal adhesions, Int J Biol Sci, 9 (2013) 966-979.
[57] D.A. Winer, H. Luck, S. Tsai, S. Winer, The Intestinal Immune System in Obesity and Insulin Resistance, Cell metabolism, 23 (2016) 413-426.
[58] E. Thursby, N. Juge, Introduction to the human gut microbiota, The Biochemical journal, 474 (2017) 1823-1836.
[59] N. Ottman, S.Y. Geerlings, S. Aalvink, W.M. de Vos, C. Belzer, Action and function of Akkermansia muciniphila in microbiome ecology, health and disease, Best Pract Res Clin Gastroenterol, 31 (2017) 637-642.
[60] C.L. Karlsson, J. Onnerfalt, J. Xu, G. Molin, S. Ahrne, K. Thorngren-Jerneck, The microbiota of the gut in preschool children with normal and excessive body weight, Obesity (Silver Spring), 20 (2012) 2257-2261.
[61] M.C. Dao, A. Everard, J. Aron-Wisnewsky, N. Sokolovska, E. Prifti, E.O. Verger, B.D. Kayser, F. Levenez, J. Chilloux, L. Hoyles, M.I.-O. Consortium, M.E. Dumas, S.W. Rizkalla, J. Dore, P.D. Cani, K. Clement, Akkermansia muciniphila and improved metabolic health during a dietary intervention in obesity: relationship with gut microbiome richness and ecology, Gut, 65 (2016) 426-436.
[62] A. Everard, C. Belzer, L. Geurts, J.P. Ouwerkerk, C. Druart, L.B. Bindels, Y. Guiot, M. Derrien, G.G. Muccioli, N.M. Delzenne, W.M. de Vos, P.D. Cani, Cross-talk between Akkermansia

muciniphila and intestinal epithelium controls diet-induced obesity, Proceedings of the National Academy of Sciences of the United States of America, 110 (2013) 9066-9071.
[63] L. Garidou, C. Pomie, P. Klopp, A. Waget, J. Charpentier, M. Aloulou, A. Giry, M. Serino, L. Stenman, S. Lahtinen, C. Dray, J.S. Iacovoni, M. Courtney, X. Collet, J. Amar, F. Servant, B. Lelouvier, P. Valet, G. Eberl, N. Fazilleau, V. Douin-Echinard, C. Heymes, R. Burcelin, The Gut Microbiota Regulates Intestinal CD4 T Cells Expressing RORgammat and Controls Metabolic Disease, Cell metabolism, 22 (2015) 100-112.
[64] A.C. Ericsson, C.E. Hagan, D.J. Davis, C.L. Franklin, Segmented filamentous bacteria: commensal microbes with potential effects on research, Comp Med, 64 (2014) 90-98.
[65] H. Yan, R. Potu, H. Lu, V. Vezzoni de Almeida, T. Stewart, D. Ragland, A. Armstrong, O. Adeola, C.H. Nakatsu, K.M. Ajuwon, Dietary fat content and fiber type modulate hind gut microbial community and metabolic markers in the pig, PloS one, 8 (2013) e59581.
[66] S.N. Heinritz, E. Weiss, M. Eklund, T. Aumiller, C.M. Heyer, S. Messner, A. Rings, S. Louis, S.C. Bischoff, R. Mosenthin, Impact of a High-Fat or High-Fiber Diet on Intestinal Microbiota and Metabolic Markers in a Pig Model, Nutrients, 8 (2016).
[67] R. Caesar, V. Tremaroli, P. Kovatcheva-Datchary, P.D. Cani, F. Backhed, Crosstalk between Gut Microbiota and Dietary Lipids Aggravates WAT Inflammation through TLR Signaling, Cell metabolism, 22 (2015) 658-668.
[68] G.D. Wu, J. Chen, C. Hoffmann, K. Bittinger, Y.Y. Chen, S.A. Keilbaugh, M. Bewtra, D. Knights, W.A. Walters, R. Knight, R. Sinha, E. Gilroy, K. Gupta, R. Baldassano, L. Nessel, H. Li, F.D. Bushman, J.D. Lewis, Linking long-term dietary patterns with gut microbial enterotypes, Science (New York, N.Y, 334 (2011) 105-108.
[69] R. Fucho, N. Casals, D. Serra, L. Herrero, Ceramides and mitochondrial fatty acid oxidation in obesity, FASEB J, 31 (2017) 1263-1272.
[70] Y.R. Kim, G. Volpert, K.O. Shin, S.Y. Kim, S.H. Shin, Y. Lee, S.H. Sung, Y.M. Lee, J.H. Ahn, Y. Pewzner-Jung, W.J. Park, A.H. Futerman, J.W. Park, Ablation of ceramide synthase 2 exacerbates dextran sodium sulphate-induced colitis in mice due to increased intestinal permeability, J Cell Mol Med, 21 (2017) 3565-3578.
[71] J. Bock, G. Liebisch, J. Schweimer, G. Schmitz, G. Rogler, Exogenous sphingomyelinase causes impaired intestinal epithelial barrier function, World J Gastroenterol, 13 (2007) 5217-5225.
[72] Y. Zhang, X. Li, K.A. Becker, E. Gulbins, Ceramide-enriched membrane domains--structure and function, Biochimica et biophysica acta, 1788 (2009) 178-183.
[73] W.J. van Blitterswijk, A.H. van der Luit, R.J. Veldman, M. Verheij, J. Borst, Ceramide: second messenger or modulator of membrane structure and dynamics?, The Biochemical journal, 369 (2003) 199-211.
[74] E. Bieberich, Sphingolipids and lipid rafts: Novel concepts and methods of analysis, Chem Phys Lipids, 216 (2018) 114-131.
[75] A. Nusrat, C.A. Parkos, P. Verkade, C.S. Foley, T.W. Liang, W. Innis-Whitehouse, K.K. Eastburn, J.L. Madara, Tight junctions are membrane microdomains, Journal of cell science, 113 (Pt 10) (2000) 1771-1781.
[76] A. Dodelet-Devillers, R. Cayrol, J. van Horssen, A.S. Haqqani, H.E. de Vries, B. Engelhardt, J. Greenwood, A. Prat, Functions of lipid raft membrane microdomains at the blood-brain barrier, J Mol Med (Berl), 87 (2009) 765-774.
[77] M.N. Perera, V. Ganesan, L.J. Siskind, Z.M. Szulc, J. Bielawski, A. Bielawska, R. Bittman, M. Colombini, Ceramide channels: influence of molecular structure on channel formation in membranes, Biochimica et biophysica acta, 1818 (2012) 1291-1301.
[78] S.J. Laulederkind, A. Bielawska, R. Raghow, Y.A. Hannun, L.R. Ballou, Ceramide induces interleukin 6 gene expression in human fibroblasts, J Exp Med, 182 (1995) 599-604.
[79] B.L. Fiebich, K. Lieb, M. Berger, J. Bauer, Stimulation of the sphingomyelin pathway induces interleukin-6 gene expression in human astrocytoma cells, J Neuroimmunol, 63 (1995) 207-211.
[80] T. Suzuki, Regulation of intestinal epithelial permeability by tight junctions, Cell Mol Life Sci, 70 (2013) 631-659.
[81] K.L. Fritsche, The science of fatty acids and inflammation, Adv Nutr, 6 (2015) 293S-301S.

[82] X. Palomer, J. Pizarro-Delgado, E. Barroso, M. Vazquez-Carrera, Palmitic and Oleic Acid: The Yin and Yang of Fatty Acids in Type 2 Diabetes Mellitus, Trends Endocrinol Metab, 29 (2018) 178-190.
[83] S. De Santis, E. Cavalcanti, M. Mastronardi, E. Jirillo, M. Chieppa, Nutritional Keys for Intestinal Barrier Modulation, Front Immunol, 6 (2015) 612.
[84] C.A. Thaiss, M. Levy, I. Grosheva, D. Zheng, E. Soffer, E. Blacher, S. Braverman, A.C. Tengeler, O. Barak, M. Elazar, R. Ben-Zeev, D. Lehavi-Regev, M.N. Katz, M. Pevsner-Fischer, A. Gertler, Z. Halpern, A. Harmelin, S. Aamar, P. Serradas, A. Grosfeld, H. Shapiro, B. Geiger, E. Elinav, Hyperglycemia drives intestinal barrier dysfunction and risk for enteric infection, Science (New York, N.Y, 359 (2018) 1376-1383.

Figure legends

Figure 1: Palm oil gavage increases intestinal permeability *in vivo*. Mice received one (1×) or five gavages (5×) with 200 µl palm oil or water. The control group was constituted of mice treated with DSS in drinking water to induce barrier damage. (**A**) Intestinal permeability after oil or water gavage was assessed by measuring plasma concentrations of FITC-dextran 1 h after oral 4 kDa FITC-dextran load. Results are expressed in µg/ml (mean ± SEM, n = 5–10). **p < 0.01, ****p < 0.0001 as compared to water. (**B**) Immunofluorescence analysis of E-cadherin, ZO-1, occludin, and tricellulin distribution in jejunum sections. Nuclei were stained with DAPI. An enlargement is shown for each condition. White arrows indicate junctional protein localization. Red arrows indicate E-cadherin and ZO-1 mislocalization. Scale bar = 20 µm. (**C**) RT-PCR determination of occludin expression in the jejunum. Cyclophilin (cyclo) was used as the reference gene. Results are expressed in arbitrary units (a.u.) as the ratio of the target gene to cyclophilin mRNA level (mean ± SEM, n = 10). *p < 0.05, ***p < 0.001 as compared to water condition.

Figure 2: Repeated gavages with palm oil modify the expression of genes involved in the immune response. Mice received one (1×) or five (5×) gavages with 200 µl palm oil or water. The control group was constituted of DSS-treated mice. The intestine was collected 1 h after the last gavage. (**A**) ELISA quantification of IL-1β protein in the colon. Results are expressed in pg/mg protein (mean ± SEM, n = 5–9). *p < 0.05, **p < 0.01 as compared to water condition. (**B**, **C**) RT-PCR determination of *Gata3* expression in the jejunum (**B**) and *Reg3g* expression in the ileum (**C**). Cyclophilin (cyclo) was used as the reference gene. Results are expressed in arbitrary units (a.u.) as the ratio of the target gene to cyclophilin mRNA level (mean ± SEM, n = 5–10).

Figure 3: **Repeated palm oil gavages modify gut bacterial species.** Mice received daily gavages with water or palm oil for four consecutive days. Total fecal DNA was extracted and used for qPCR quantification of bacterial species content. Results are expressed as the mean ± SEM (n = 4–6), *p < 0.05 as compared to water; ns: not statistically significant; a.u.: arbitrary unit. Fecal quantification of (**A**) *Clostridium leptum*, (**B**) *Akkermansia muciniphila*, (**C**) segmented filamentous bacteria, (**D**) *Bacteroides* sp., (**E**) *Lactobacillus* sp., and (**F**) *Clostridium coccoides*. (**G**) Total fecal bacterial counts.

Figure 4: Saturated palmitic acid but not unsaturated oleic acid increases the paracellular permeability of the intestinal epithelial monolayer. Caco-2/TC7 cells were incubated with control medium (Ctrl) or were treated with palmitic acid (PA) or oleic acid (OA) micelles for 24h or daily for four consecutive days (4d). The positive control was 24-h treatment with 4.5 mM EGTA. (**A**) Paracellular permeability across the Caco-2/TC7 cell monolayer was evaluated by measuring the accumulation during 4-h exposure to 4 kDa FITC-dextran in the basal compartment. Results are

expressed as the percentage of 4 kDa FITC-dextran input (amount added in the apical compartment) (mean ± SEM, n = 6–15). Fold increase, as compared to the control condition, is indicated at the top of the corresponding histogram. **p < 0.01, ***p < 0.001 as compared to control (Ctrl) cells. (**B**) Dose–response to palmitic acid was evaluated on cells incubated for 4 days with micelles containing 0.1 mM, 0.3 mM, or 0.6 mM palmitic acid (PA). The accumulation of 4 kDA FITC-dextran in the basal compartment was determined. Results are expressed as in (A) (mean ± SEM, n = 6). **p < 0.01, ***p < 0.001 as compared to control (Ctrl) cells. (**C**) TEER (inverse relationship to permeability) was assessed in the control and EGTA-treated cells. Results are expressed in percentage of TEER measured in control condition (mean ± SEM, n = 6). The percentage of decrease compared to the control condition is indicated. (**D**) The time course of TEER was measured before (0 h) and every 24 h during treatment with palmitic acid (PA) or oleic acid (OA) micelles or in untreated cells (control). The percentage of decrease in PA-treated cells as compared to control cells is indicated. Results are expressed in ohm.cm^2 as mean ± SEM (n = 6). *p < 0.05, **p < 0.01, ***p < 0.001 as compared to untreated cells, unless otherwise indicated. (**E**) Dose–response of TEER was assessed in control and in cells treated for 4 days with micelles containing 0.1 mM, 0.3 mM, or 0.6 mM palmitic acid. Results are expressed as in (D) (mean ± SEM, n = 6). *p < 0.05, ***p < 0.001 as compared to control cells.

Figure 5: Repeated supply of palmitic acid, but not oleic acid, alters the expression of junctional proteins and their localization at cell–cell contacts. Cells were incubated with or without micelles containing palmitic acid (PA) (for 24 h or 4 days [4d]) or oleic acid (OA) (for 4 days [4d]). (**A**) Immunofluorescence analysis was performed to study E-cadherin, ZO-1, occludin, and tricellulin localization. Nuclei were stained with DAPI. Bar = 20 μm. (**B**) Western blot determination of protein levels in cell lysates. Reconstituted images are shown. Hsc70 protein levels were used as loading controls. (**C–F**) Quantification of junctional protein levels normalized to Hsc70 protein levels. Results are expressed in arbitrary units (a.u.) (mean ± SEM, n = 4), *p < 0.05, **p < 0.001 as compared to control (Ctrl). (**G**) RT-PCR quantification of occludin mRNA levels. Cyclophilin (cyclo) was used as the reference gene. Results are expressed in arbitrary units (a.u.) as the ratio of the target gene to cyclophilin mRNA level (mean ± SEM, n = 6–15).

Figure 6: Palmitic acid modifies cytokine expression in Caco-2/TC7 cells. Caco-2/TC7 cells were cultured in the same conditions as in Figure 4. The mRNA levels of *IL8* (**A**), *TGFB1* (**C**), and *IL1B* (**D**), were quantified by RT-PCR. Cyclophilin (cyclo) was used as the reference gene. Results are expressed in arbitrary units (a.u.) as the ratio of the target gene to cyclophilin mRNA level (mean ± SEM, n = 6–15). (**B**) ELISA quantification of the concentration of IL-8 protein in the basal compartment. Results are expressed in pg/ml (mean ± SEM, n = 6). Fold increase as compared to control condition is indicated at the top of histograms. (**E**, **F**) Dose–response to palmitic acid on mRNA levels of *IL8* (**E**) and *TGFB1* (**F**). Cells were incubated for 4 days with micelles containing 0.1

mM, 0.3 mM, or 0.6 mM palmitic acid (PA). The mRNA levels were quantified by RT-PCR. Cyclophilin (cyclo) was used as the reference gene. Results are expressed in arbitrary units (a.u.) as the ratio of the target gene to cyclophilin mRNA level (mean ± SEM, n = 4). (**G**) Dose–response to palmitic acid on IL-8 secretion was determined as in (B). *p < 0.05, **p < 0.01, ***p < 0.001, ****p < 0.0001 as compared to control.

Figure 7: Removing of palmitic acid partially restores its deleterious effects on intestinal epithelial cell monolayer integrity and on the expression of genes involved in immune response. Caco-2/TC7 cells were cultured in control medium (Ctrl) or with palmitic acid micelles (PA) for 4 days followed with or without one or two more days in control medium without PA (w/o PA). (**A**) Paracellular permeability was evaluated by measuring 4 kDa FITC-dextran flux across the Caco-2/TC7 monolayer after 4-day palmitic acid treatment and each day after cells were shifted to control medium. The 4 kDa FITC-dextran was added in the apical compartment and fluorescence values were determined in the basal compartment 4 h later. Results are expressed as the percentage of 4 kDa FITC-dextran input in the apical compartment (mean ± SEM, n = 6–18). Fold increase, as compared to control condition, is indicated at the top of histograms. *p < 0.05, **p < 0.01, ***p < 0.001 as compared to control cells on the same day of culture, unless otherwise indicated. (**B**) TEER was measured in control (white circles) and palmitic acid–treated cells (black circles). The measurement was performed before treatment (day 0), at day 1 and 4 of palmitic acid treatment, and after removing the palmitic acid micelles (grey circles). Dashed line indicates the day PA-treated cells were shifted to control medium. Results are expressed in ohm.cm^2 (mean ± SEM, n = 6–18). The percentage of decrease in PA-treated cells as compared to control cells is indicated. **p < 0.01, ***p < 0.001 as compared to control cells. (**C**) Immunofluorescence analysis was performed to study E-cadherin, ZO-1, occludin, and tricellulin localization. Nuclei were stained with DAPI. Bar = 20 μm. (**D**) Western blot measurement of occludin and tricellulin protein levels. Reconstituted images are shown. Actin was used as the loading control. (**E**–**G**) RT-PCR quantification of the mRNA levels of *OCLN* (**E**), *IL8* (**F**), and *TGFB1* (**G**). Cyclophilin (cyclo) was used as the reference gene. Results are expressed in arbitrary units (a.u.) as the ratio of the target gene to cyclophilin mRNA level (mean ± SEM, n = 6–18). *p < 0.05, **p < 0.01 as compared to control, unless otherwise indicated; ns: not statistically significant.

Figure 8: Palmitic acid provokes moderate ER stress in Caco-2/TC7 cells. Caco-2/TC7 cells were incubated with control medium (Ctrl) or were treated for 24 h or daily for four consecutive days (4 d) with palmitic acid (PA) or oleic acid (OA) micelles. The positive control was 4-h treatment with 2 mM DTT. (**A**) Paracellular permeability was evaluated by measuring 4 kDa FITC-dextran flux across the Caco-2/TC7 cell monolayer. The 4 kDa FITC-dextran was added in the apical compartment on the last day of the experiment, and fluorescence values were determined in the basal compartment 4 h later. Results are expressed in percentage of 4 kDa FITC-dextran added in the apical compartment

(input) (mean ± SEM, n = 4–6). (**B**–**E**) RT-PCR quantification of the mRNA levels of *IL8* (**B**) *GRP78*/*HSPA5* (**C**), *GADD153*/*DDIT3* (**D**), and *XBP1* spliced form (**E**). Cyclophilin (cyclo) was used as the reference gene. Results are expressed in arbitrary units (a.u.) as the ratio of the target gene to cyclophilin mRNA level (mean ± SEM, n = 6–15). Fold increase as compared to control condition is indicated at the top of some histograms. *p < 0.05, **p < 0.01, ***p < 0.01, ****p < 0.0001 as compared to control.

Figure 9: C_2-ceramide addition provokes barrier defects and modulates cytokine expression. Caco-2/TC7 cells were cultured for 24 h in the absence (Ctrl) or presence of vehicle 0.5% ethanol (EtOH) or 100 μM C_2-ceramide (C_2-Cer). (**A**) Paracellular permeability was evaluated by measuring 4 kDa FITC-dextran flux across the Caco-2/TC7 cell monolayer as in Figure 4. Results are expressed as percentage of 4 kDa FITC-dextran input in the apical compartment (mean ± SEM, n = 6). (**B**) TEER was measured after the 24-h treatment. Results are expressed in % of value obtained in untreated cells (mean ± SEM, n = 6). (**C**) Representative western blots of junction protein levels determined in cell lysates. Reconstituted images are shown. Hsc70 was used as the loading control. (**D**) Immunofluorescence analysis of Caco-2/TC7 cells for ZO-1, occludin, tricellulin, and E-cadherin. Nuclei were stained with DAPI. Bar = 20 μm. (**E**, **G**, **H**) RT-PCR quantification of the mRNA levels of *IL8* (**E**), *TGFB1* (**G**), and *IL1B* (**H**). Cyclophilin (cyclo) was used as the reference gene. Results are expressed in arbitrary units (a.u.) as the ratio of the target gene to cyclophilin mRNA level (mean ± SEM, n = 6–15). (**F**) ELISA quantification of the concentration of IL-8 protein in the basal compartment. Results are expressed in pg/ml (mean ± SEM, n = 6). *p < 0.05, **p < 0.01, ***p < 0.01, ****p < 0.0001 as compared to untreated cells.

Figure 10: Inhibition *of de novo* ceramide synthesis abolishes inflammatory effects of palmitic acid. Caco-2/TC7 cells were cultured for 24 h in the absence (Ctrl) or presence of palmitic acid (PA) micelles or 20 mM L-cycloserine (Lcyclo). In one condition, cells were pre-treated with L-cycloserine for 1 h before 24-h incubation with PA micelles (PA+Lcyclo). (**A**) Paracellular permeability was evaluated by measuring 4 kDa FITC-dextran flux across the Caco-2/TC7 cell monolayer. Results are expressed in percentage of 4 kDa FITC-dextran input in the apical compartment (mean ± SEM, n = 3–6). (**B**) RT-PCR quantification of *IL8* mRNA levels. Cyclophilin (cyclo) was used as the reference gene. Results are expressed in arbitrary units (a.u.) as the ratio of *IL8* mRNA level to cyclophilin mRNA level (mean ± SEM, n = 3–6). **p < 0.01, ***p < 0.001 as compared to control cells unless indicated; ns: not statistically significant.

Figure 11: Schematic representation of palmitic acid and palm oil effects in intestinal cells.
Left: In mice, one palm oil bolus is sufficient to alter cell junctions and to increase intestinal permeability to macromolecules. The increased expression of *Reg3g*, an antimicrobial peptide,

suggests that the intestine engages the mucosal defense. Additional gut alterations are detected after repeated palm oil gavages: The increased *Reg3g* expression observed after a single palm oil bolus is no longer observed after repeated supply, suggesting that the antimicrobial host defense is lost or less effective in this condition. Expression of IL-1β is increased in the colon; decreased expression of *Gata3* is observed in the jejunum. Moreover, changes in bacterial species composition of the microbiota, i.e., *C. leptum*, *A. muciniphila*, segmented filamentous bacteria, and *Bacteroides* sp., are identified. Altogether, these results show that intestinal epithelial barrier disruption is an early event triggered by palm oil and that short-term supply of dietary lipids initiates the intestinal inflammatory response and provoke changes in microbiota composition.

Right: In human epithelial cells, palmitic acid, supplied as micelles, disrupts cell junctions, increases paracellular permeability, and induces IL-8 expression and secretion. Ceramide production from palmitic acid controls IL-8 expression and participates in epithelial barrier disruption. Altogether, these results show that palmitic acid exerts direct effects on the epithelial compartment, where it initiates the inflammatory response.

We hypothesize that, in response to palm oil or palmitic acid, IL-1β and IL-8 contribute to tight junction defects and amplify intestinal hyperpermeability. It is not known whether the initiation of intestinal inflammation by dietary lipids before the onset of diet-induced obesity can lead to low-grade systemic inflammation.

Table 1: Primer sequences and bacteria strains used used for the quantification of bacterai group or species

group or species	forward primer		reverse primer		bacteria strain used for the standard curve
	name	sequence	name	sequence	
Clostridium leptum	Clept 09	5'-CCTTCCGTCCGSAGTTA-3'	Clept 08	5'-GAATTAAACACAT CTCACTGCTT-3'	*Faecalibacterium prausnitzii*
Akkermansia muciniphila	AKK-F	5'-GGTAGCCGGTCTGAGAGGAT-3'	AKK-R	5'-TAGGTGTCTGGACCGTGTCTC-3'	see legend below
Lactobacillus sp.	Lacto 04	5'-CGCCACTGGTGTTCYTCCATA-3'	Lacto 05	5'-AGCAGTAGGGAATCTTCCA-3'	*Lactobacillus acidophilus*
Segmented Filamentous Bacteria	SFB-F	5'-CACGGTCCATACTCCTACGG-3'	SFB-R	5'-AGGGTTTCCCCCATTGTG-3'	see legend below
Bacteroides sp.	Bacter 11	5'-CCTWCGATGGATAGGGGTT-3'	Bacter 08	5'-CACGCTACTTGGCTGGTTCAG-3'	*Bacteroides thetaiotaomicron*
Clostridium coccoides	Ccoc 07	5'-GACGCCGCGTGAAGGA-3'	Ccoc 14	5'-AGCCCCAGCCTTTCACATC-3'	*Clostridium coccoides*
All bacteria	F_Bact 1369	5'-CGGTGAATACGTTCCCGG-3'	R_PROK 1492	5'-TACGGCTACCTTGTTACGACTT-3'	*Escherichia coli*

The determination of *Akkermansia muciniphila* and Segmented Filamentous Bacteria abundance was determined by relative quantification to a control sample.

Table 2: List of primer sequences used for RT-PCR analyses

human genes (alias names)	forward primer	reverse primer
CXCL8 (IL-8)	5'-AGACAGCAGAGCACACAAGC-3'	5'-ATGGTTCCTTCCGGTGGT-3'
TGFB1 (TGF-Beta-1)	5'-GCAGCACGTGGAGCTGTA-3'	5'-CAGCCGGTTGCTGAGGTA-3'
IL1B (IL-1-Beta)	5'-CTGTCCTGCGTGTTGAAAGA-3'	5'-TTGGGTAATTTTTGGGATCTACA-3'
HSPA5 (GRP78, BIP)	5'-CTGGGTACATTTGATCTGACTGG-3'	5'-TCCTTGAGCTTTTTGTCTTCCT-3'
DDIT3 (GADD153, CHOP)	5'-AGCTGTGCCACTTTCCTTTC-3'	5'-CAGAACCAGAGAGGTCACA-3'
XBP1 spliced form	5′-TGCTGAGTCCGCAGCAGGTG-3′	5'-GCTGGCAGGCTCTGGGGAAG-3′
PPIB (Cyclophilin B)*	5'-GCCTTAGCTACAGGAGAGAA-3'	5'-TTTCCTCCTGTGCCATCTC-3'
CDH1 (e-cadherin)	5'-GCCGAGAGCTACACGTTCA-3'	5'-GACCGGTGCAATCTTCAAA-3'
TJP1 (ZO-1)	5'-CAGAGCCTTCTGATCATTCCA-3'	5'-CATCTCTACTCCGGAGACTGC-3'
OCLN (occludin)	5'-AGGAACCGAGAGCCAGGT-3'	5'-GGATGAGCAATGCCCTTTAG-3'
MARVELD2 (tricellulin)	5'-CAGGCTGTCCTGAGGAAGTT-3'	5'-CCGAATGATGTGGCAATCT-3'

mouse genes	forward primer	reverse primer
Cdh1 (e-cadherin)	5'-TCCTTGTTCGGCTATGTGTC-3'	GGCATGCACCTAAGAATCAG
Tjp1 (ZO-1)	5'-AGGACACCAAAGCATGTGAG-3'	5'-GGCATTCCTGCTGGTTACA-3'
Ocln (occludin)	5'-TCCGTGAGGCCTTTTGAA-3'	5'-GGTGCATAATGATTGGGTTTG-3'
Marveld2 (tricellulin)	5'-AGGCTCCCACATCATTCTGA-3'	5'-TCCAGAAACGAAGGGTCATT-3'
Gata3	5'-TTATCAAGCCCAAGCGAAG-3'	5'-TGGTGGTGGTCTGACAGTTC-3'
Reg3g	5'-ACCATCACCATCATGTCCTG-3'	5'-GGCATCTTTCTTGGCAACTT-3'

* PPIB gene is used as reference gene and the same sequences are used for both human and mouse species.

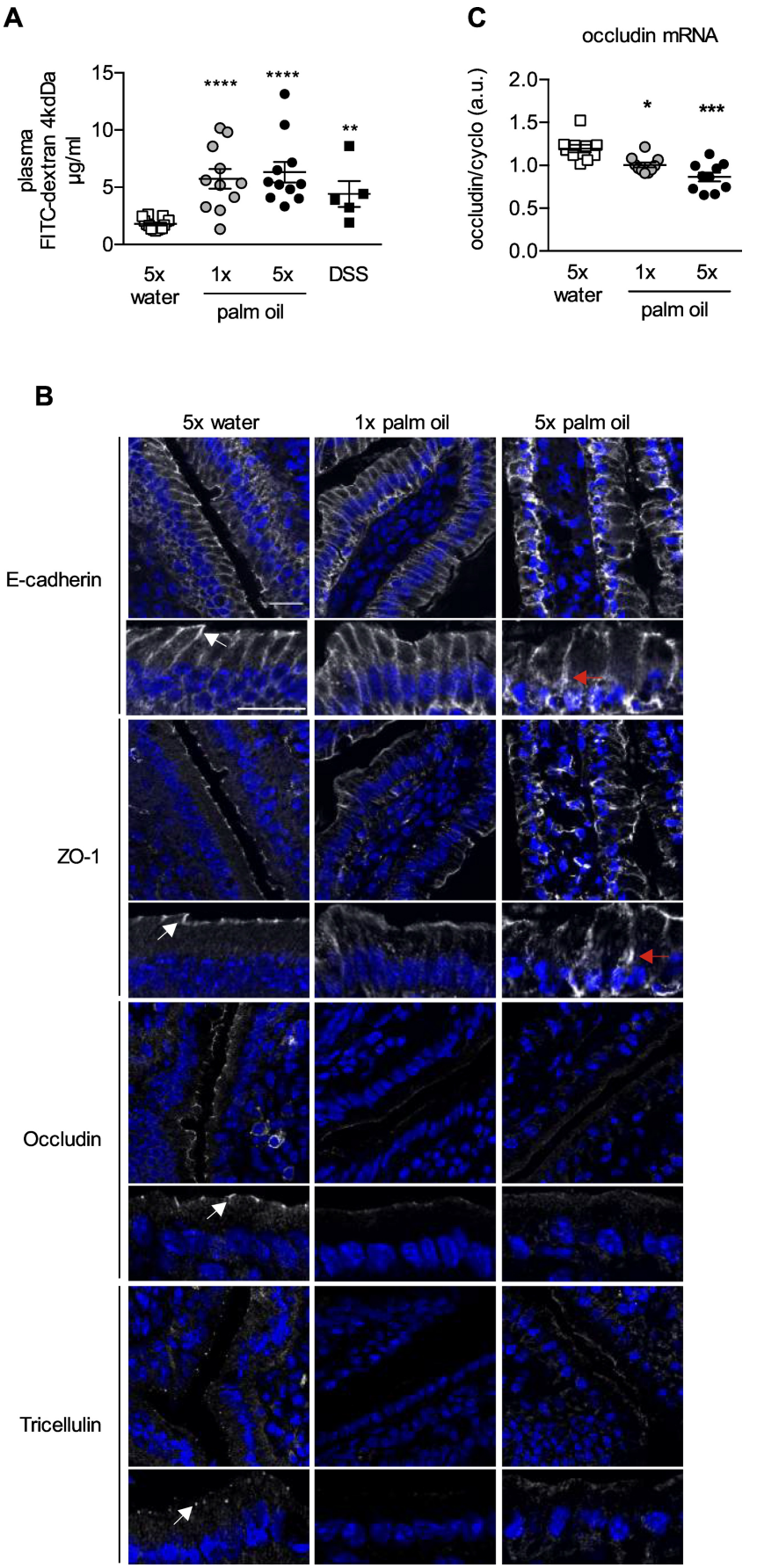
A
plasma FITC-dextran 4kdDa µg/ml
15
10
5
0
****
****
**
5x water
1x
5x
palm oil
DSS
C
occludin mRNA
occludin/cyclo (a.u.)
2.0
1.5
1.0
0.5
0.0
*
***
5x water
1x
5x
palm oil
B
5x water
1x palm oil
5x palm oil
E-cadherin
ZO-1
Occludin
Tricellulin

Figure 1

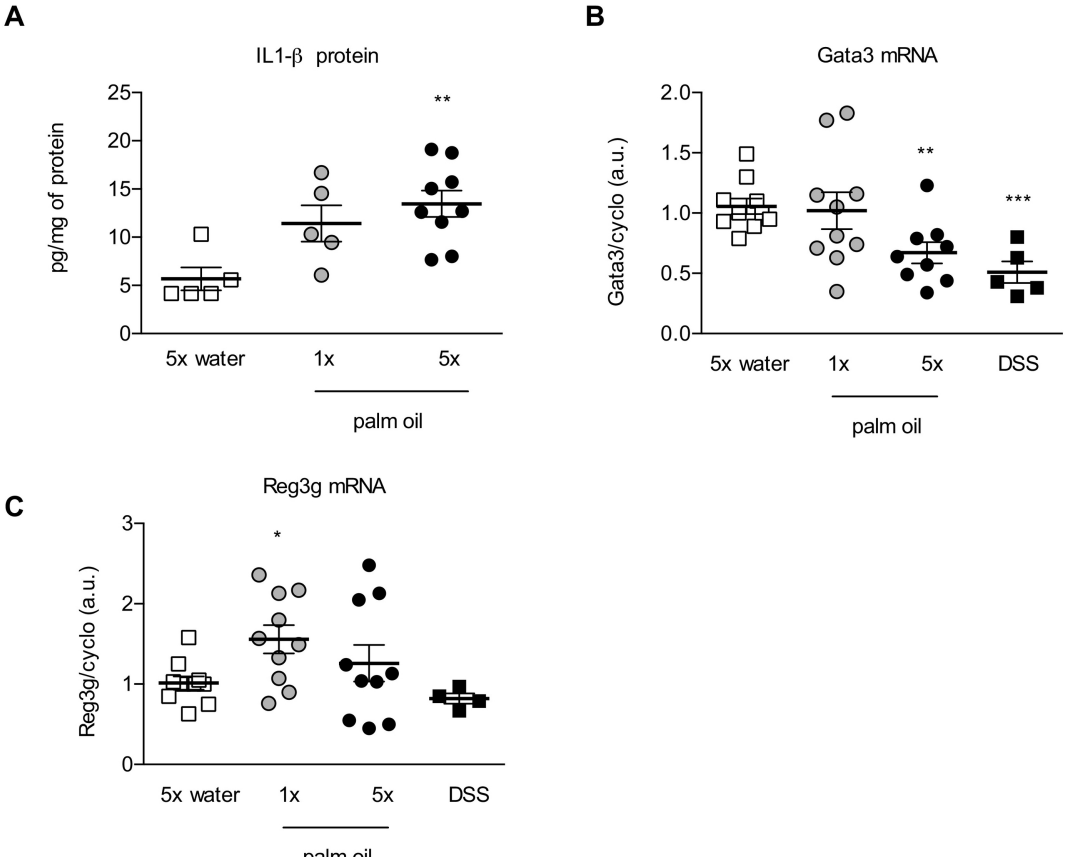
A
IL1-β protein
pg/mg of protein
25
20
15
10
5
0
**
5x water
1x
5x
palm oil
B
Gata3 mRNA
Gata3/cyclo (a.u.)
2.0
1.5
1.0
0.5
0.0
**
***
5x water
1x
5x
DSS
palm oil
C
Reg3g mRNA
Reg3g/cyclo (a.u.)
3
2
1
0
*
5x water
1x
5x
DSS
palm oil

Figure 2

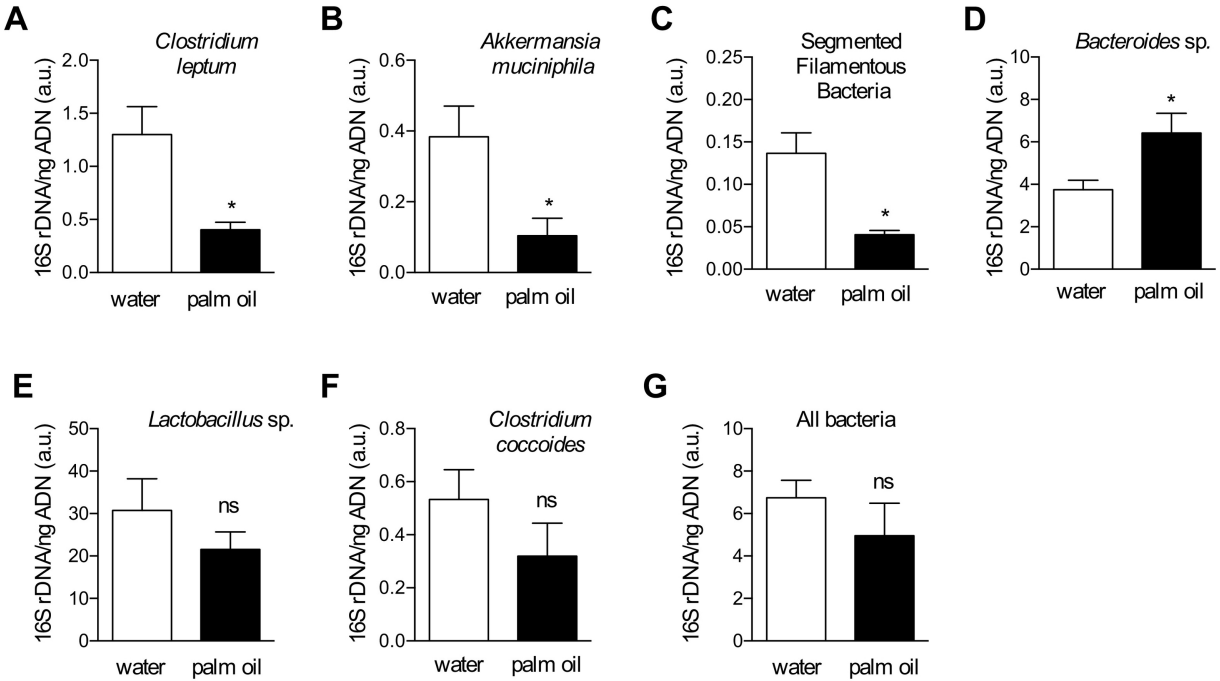
A
Clostridium leptum
16S rDNA/ng ADN (a.u.)
2.0
1.5
1.0
0.5
0.0
*
water
palm oil
B
Akkermansia muciniphila
16S rDNA/ng ADN (a.u.)
0.6
0.4
0.2
0.0
*
water
palm oil
C
Segmented Filamentous Bacteria
16S rDNA/ng ADN (a.u.)
0.25
0.20
0.15
0.10
0.05
0.00
*
water
palm oil
D
Bacteroides sp.
16S rDNA/ng ADN (a.u.)
10
8
6
4
2
0
*
water
palm oil
E
Lactobacillus sp.
16S rDNA/ng ADN (a.u.)
50
40
30
20
10
0
ns
water
palm oil
F
Clostridium coccoides
16S rDNA/ng ADN (a.u.)
0.8
0.6
0.4
0.2
0.0
ns
water
palm oil
G
All bacteria
16S rDNA/ng ADN (a.u.)
10
8
6
4
2
0
ns
water
palm oil

Figure 3

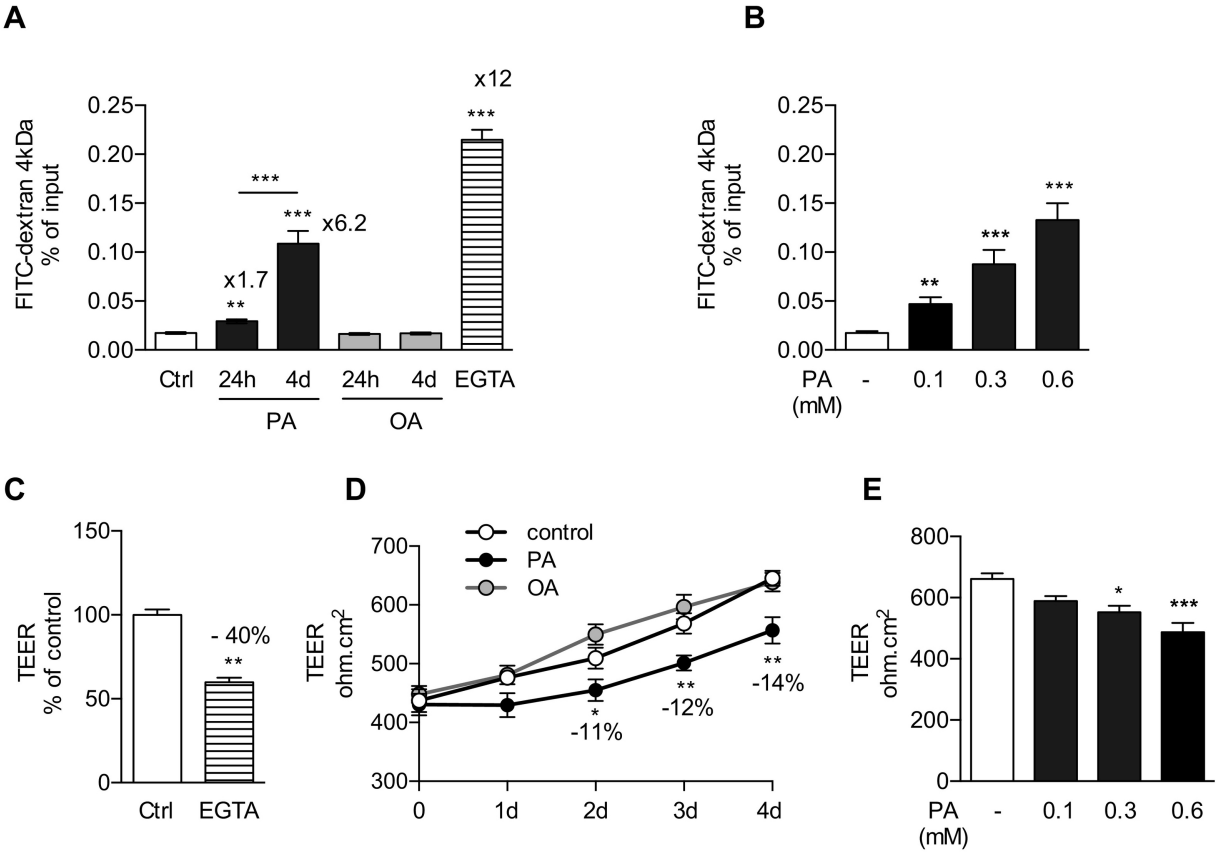
A
FITC-dextran 4kDa
% of input
0.25
0.20
0.15
0.10
0.05
0.00
x12
***
***
***
x6.2
x1.7
**
Ctrl
24h
4d
24h
4d
EGTA
PA
OA
B
FITC-dextran 4kDa
% of input
0.25
0.20
0.15
0.10
0.05
0.00
**
***
***
PA
(mM)
-
0.1
0.3
0.6
C
TEER
% of control
150
100
50
0
- 40%
**
Ctrl
EGTA
D
TEER
ohm.cm2
700
600
500
400
300
control
PA
OA
*
-11%
**
-12%
**
-14%
0
1d
2d
3d
4d
E
TEER
ohm.cm2
800
600
400
200
0
*
***
PA
(mM)
-
0.1
0.3
0.6

Figure 4

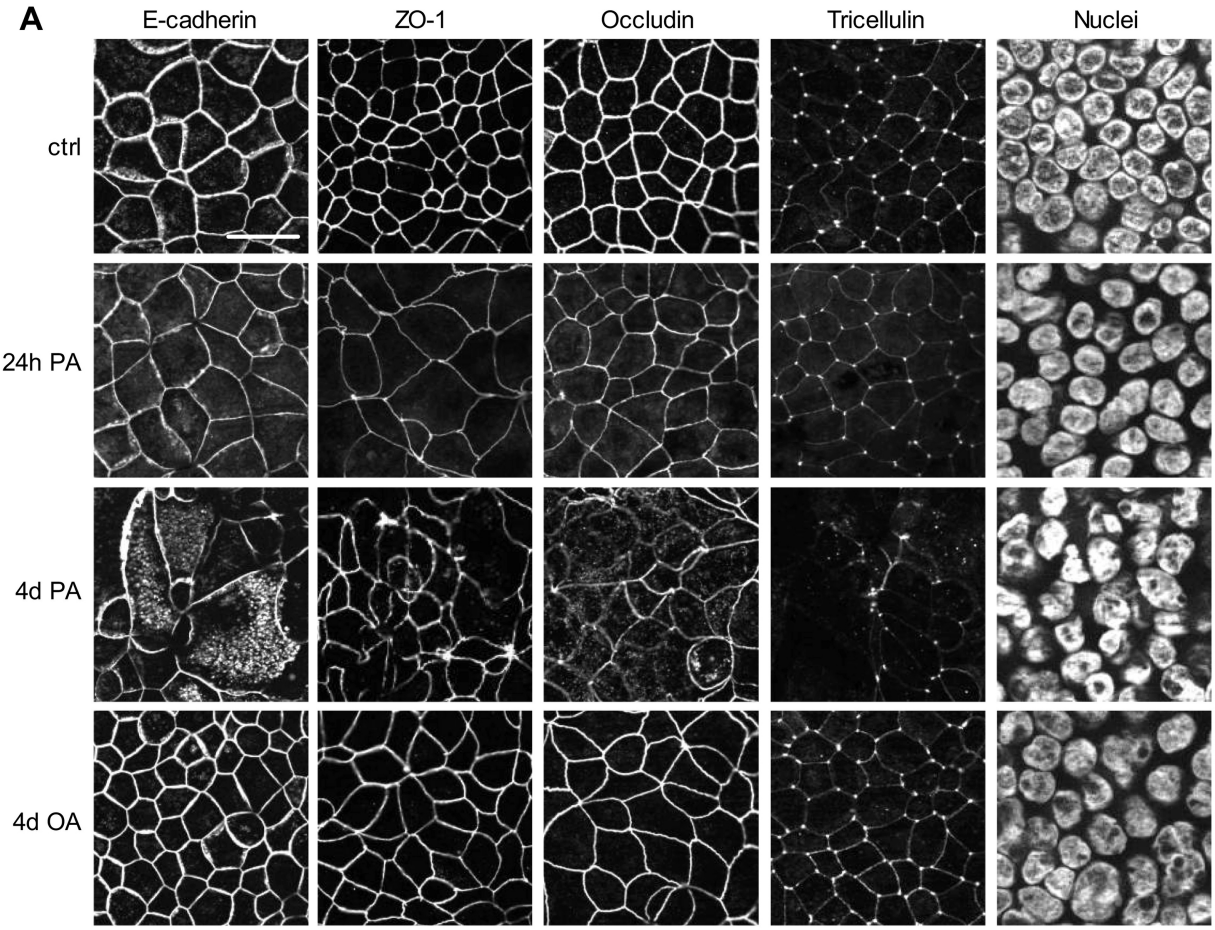
A
E-cadherin
ZO-1
Occludin
Tricellulin
Nuclei
ctrl
24h PA
4d PA
4d OA

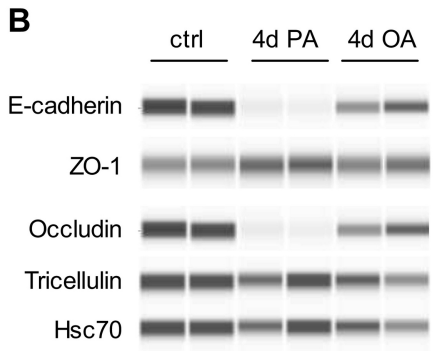
B
ctrl
4d PA
4d OA
E-cadherin
ZO-1
Occludin
Tricellulin
Hsc70

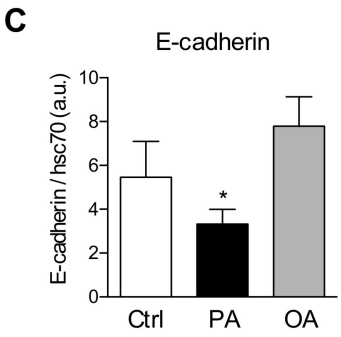
C
E-cadherin
E-cadherin / hsc70 (a.u.)
Ctrl
PA
OA

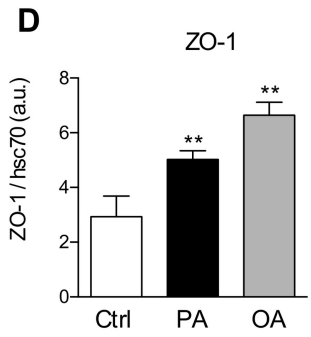
D
ZO-1
ZO-1 / hsc70 (a.u.)
Ctrl
PA
OA

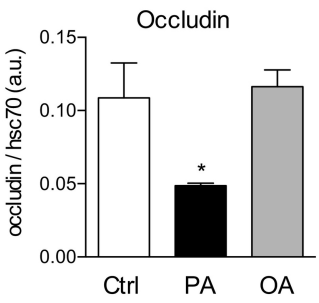
E
Occludin
occludin / hsc70 (a.u.)
Ctrl
PA
OA

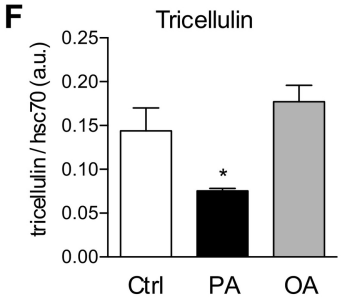
F
Tricellulin
tricellulin / hsc70 (a.u.)
Ctrl
PA
OA

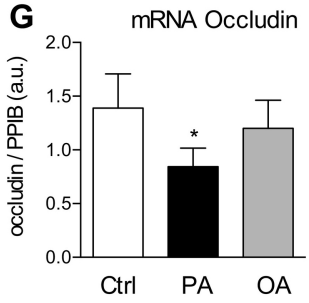
G
mRNA Occludin
occludin / PPIB (a.u.)
Ctrl
PA
OA

Figure 5

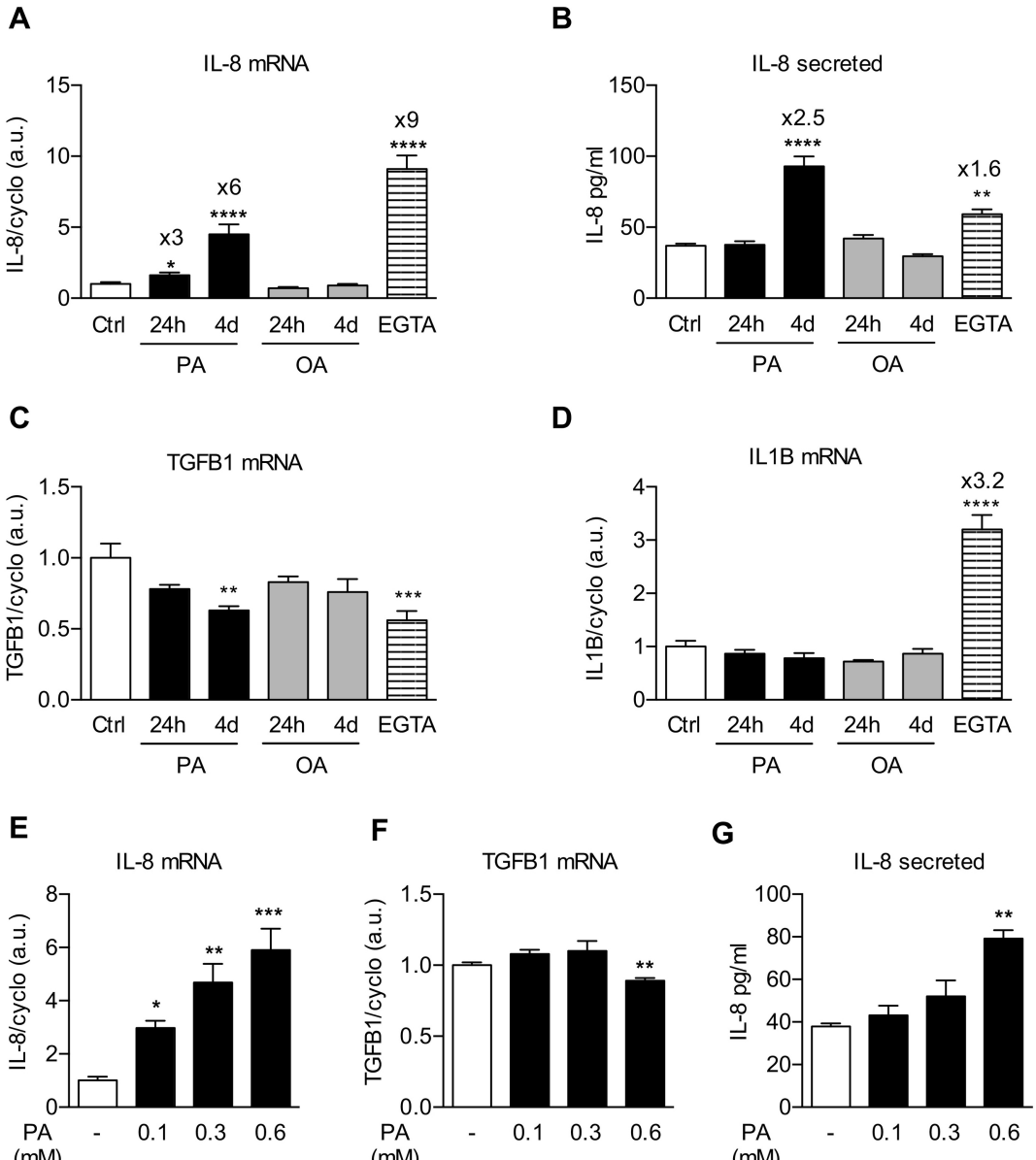
A
IL-8 mRNA
IL-8/cyclo (a.u.)
15
10
5
0
x3
*
x6
****
x9
****
Ctrl
24h
4d
24h
4d
EGTA
PA
OA
B
IL-8 secreted
IL-8 pg/ml
150
100
50
0
x2.5
****
x1.6
**
Ctrl
24h
4d
24h
4d
EGTA
PA
OA
C
TGFB1 mRNA
TGFB1/cyclo (a.u.)
1.5
1.0
0.5
0.0
**
***
Ctrl
24h
4d
24h
4d
EGTA
PA
OA
D
IL1B mRNA
IL1B/cyclo (a.u.)
4
3
2
1
0
x3.2
****
Ctrl
24h
4d
24h
4d
EGTA
PA
OA
E
IL-8 mRNA
IL-8/cyclo (a.u.)
8
6
4
2
0
*
**
***
PA
(mM)
-
0.1
0.3
0.6
F
TGFB1 mRNA
TGFB1/cyclo (a.u.)
1.5
1.0
0.5
0.0
**
PA
(mM)
-
0.1
0.3
0.6
G
IL-8 secreted
IL-8 pg/ml
100
80
60
40
20
0
**
PA
(mM)
-
0.1
0.3
0.6

Figure 6

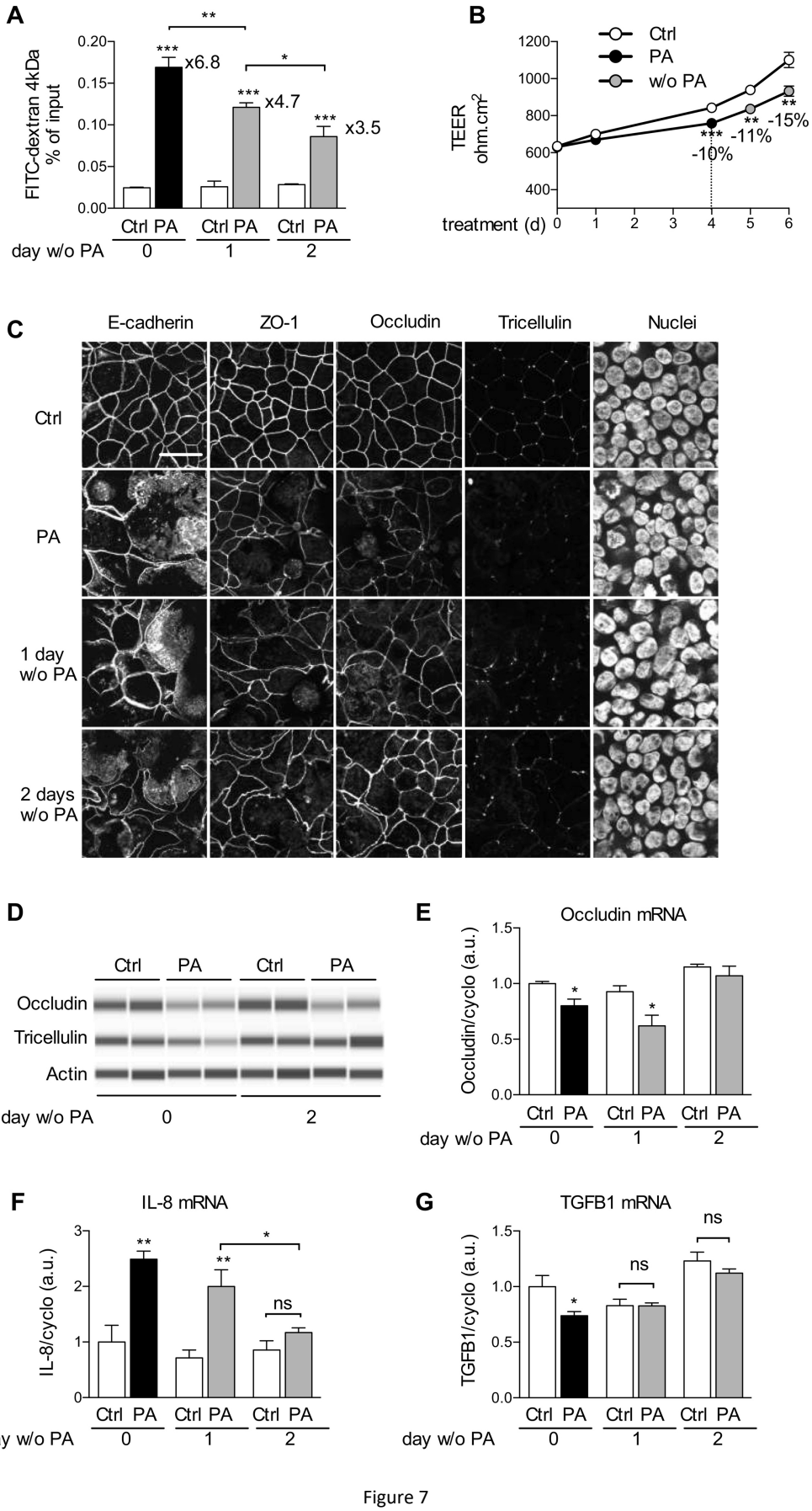
A
FITC-dextran 4kDa
% of input
0.20
0.15
0.10
0.05
0.00
**
*
***
x6.8
***
x4.7
***
x3.5
Ctrl PA Ctrl PA Ctrl PA
day w/o PA
0
1
2
B
TEER
ohm.cm2
1200
1000
800
600
400
Ctrl
PA
w/o PA
***
-11%
**
-15%
**
-10%
treatment (d)
0 1 2 3 4 5 6
C
E-cadherin
ZO-1
Occludin
Tricellulin
Nuclei
Ctrl
PA
1 day
w/o PA
2 days
w/o PA
D
Ctrl
PA
Ctrl
PA
Occludin
Tricellulin
Actin
day w/o PA
0
2
E
Occludin mRNA
Occludin/cyclo (a.u.)
1.5
1.0
0.5
0.0
*
*
Ctrl PA Ctrl PA Ctrl PA
day w/o PA
0
1
2
F
IL-8 mRNA
IL-8/cyclo (a.u.)
3
2
1
0
**
**
*
ns
Ctrl PA Ctrl PA Ctrl PA
day w/o PA
0
1
2
G
TGFB1 mRNA
TGFB1/cyclo (a.u.)
1.5
1.0
0.5
0.0
*
ns
ns
Ctrl PA Ctrl PA Ctrl PA
day w/o PA
0
1
2

Figure 7

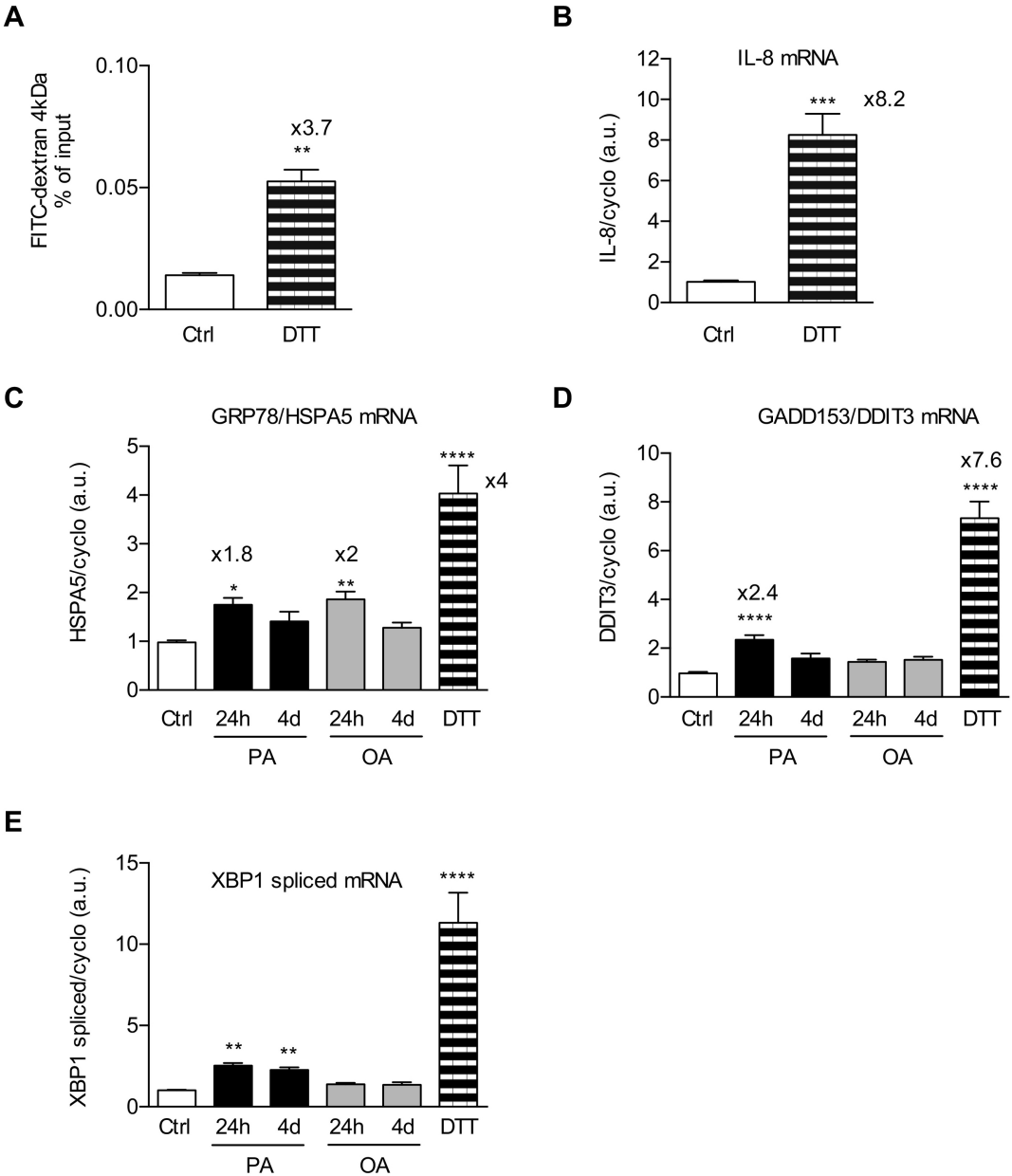
A
FITC-dextran 4kDa
% of input
0.10
0.05
0.00
x3.7
**
Ctrl
DTT
B
IL-8 mRNA
IL-8/cyclo (a.u.)
12
10
8
6
4
2
0
***
x8.2
Ctrl
DTT
C
GRP78/HSPA5 mRNA
HSPA5/cyclo (a.u.)
5
4
3
2
1
0
x1.8
*
x2
**
****
x4
Ctrl
24h
4d
24h
4d
DTT
PA
OA
D
GADD153/DDIT3 mRNA
DDIT3/cyclo (a.u.)
10
8
6
4
2
0
x2.4
****
x7.6
****
Ctrl
24h
4d
24h
4d
DTT
PA
OA
E
XBP1 spliced mRNA
XBP1 spliced/cyclo (a.u.)
15
10
5
0
**
**
****
Ctrl
24h
4d
24h
4d
DTT
PA
OA

Figure 8

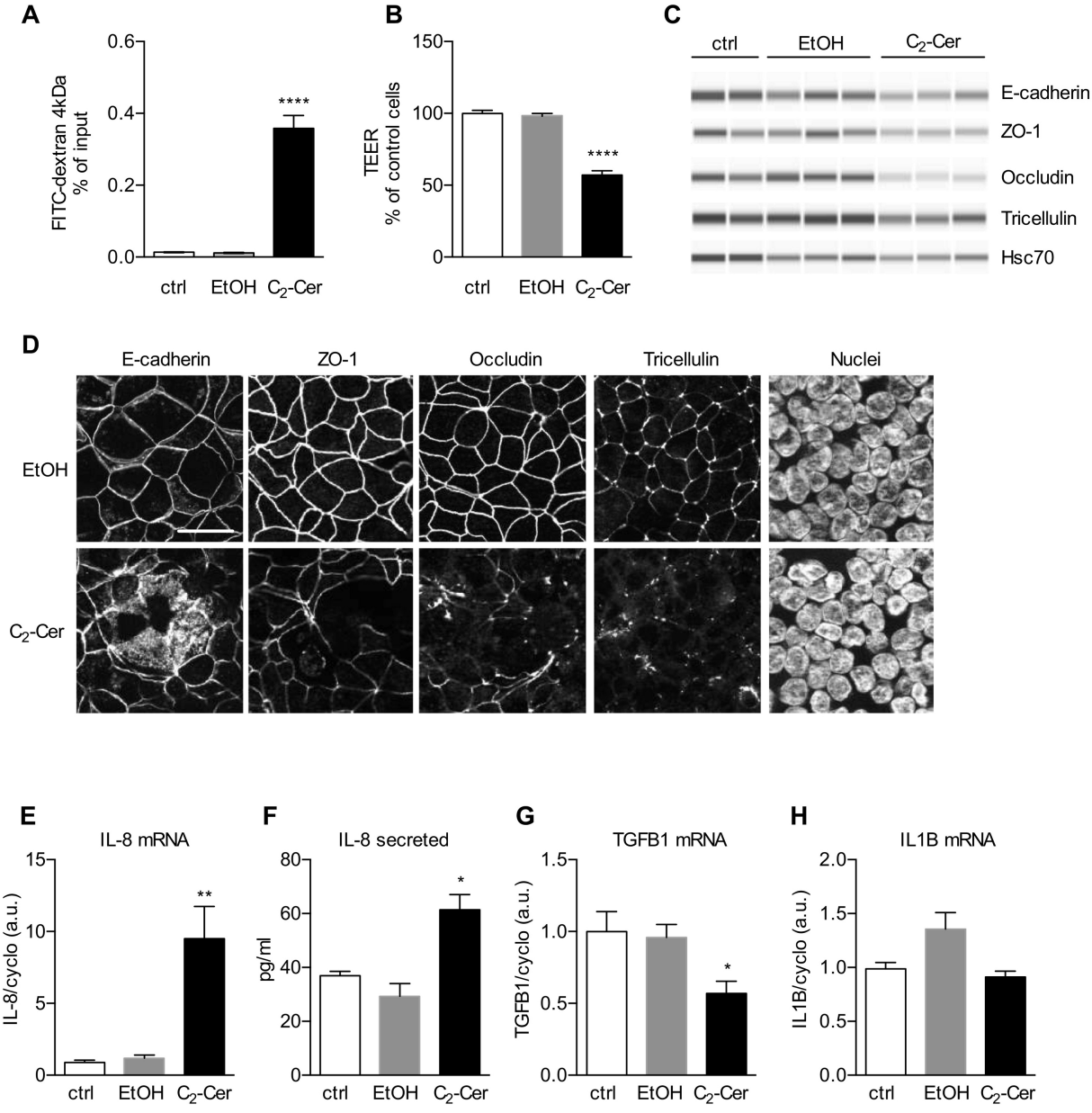
A
FITC-dextran 4kDa
% of input
0.6
0.4
0.2
0.0
****
ctrl
EtOH
C2-Cer
B
TEER
% of control cells
150
100
50
0
****
ctrl
EtOH
C2-Cer
C
ctrl
EtOH
C2-Cer
E-cadherin
ZO-1
Occludin
Tricellulin
Hsc70
D
E-cadherin
ZO-1
Occludin
Tricellulin
Nuclei
EtOH
C2-Cer
E
IL-8 mRNA
IL-8/cyclo (a.u.)
15
10
5
0
**
ctrl
EtOH
C2-Cer
F
IL-8 secreted
pg/ml
80
60
40
20
0
*
ctrl
EtOH
C2-Cer
G
TGFB1 mRNA
TGFB1/cyclo (a.u.)
1.5
1.0
0.5
0.0
*
ctrl
EtOH
C2-Cer
H
IL1B mRNA
IL1B/cyclo (a.u.)
2.0
1.5
1.0
0.5
0.0
ctrl
EtOH
C2-Cer

Figure 9

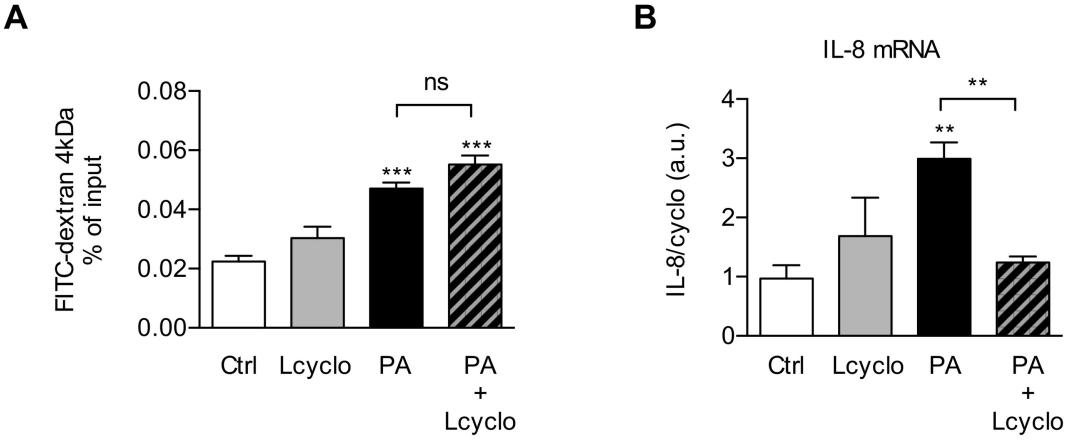
A
FITC-dextran 4kDa
% of input
0.08
0.06
0.04
0.02
0.00
ns
***
***
Ctrl
Lcyclo
PA
PA
+
Lcyclo
B
IL-8 mRNA
IL-8/cyclo (a.u.)
4
3
2
1
0
**
**
Ctrl
Lcyclo
PA
PA
+
Lcyclo

Figure 10

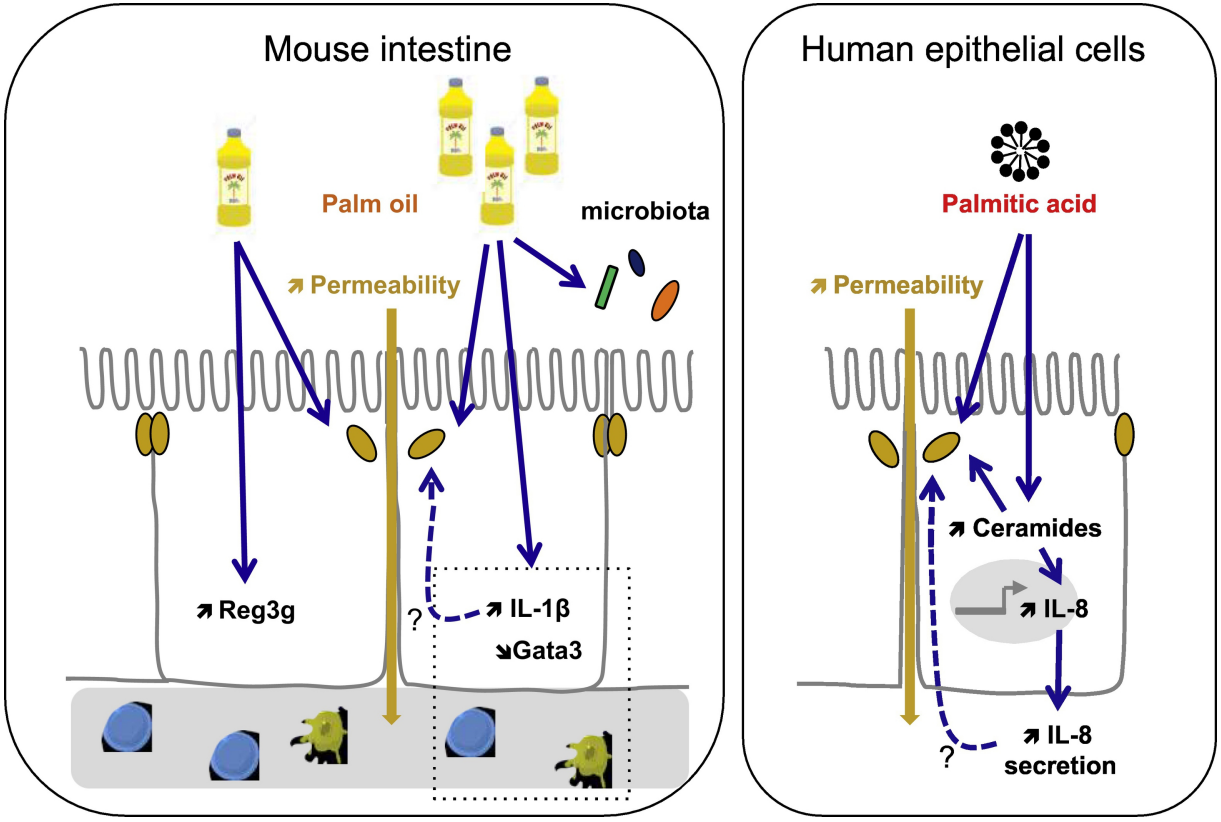
Mouse intestine
Palm oil
microbiota
Permeability
Reg3g
?
IL-1β
Gata3
Human epithelial cells
Palmitic acid
Permeability
Ceramides
IL-8
IL-8
secretion
?

Figure 11